

# Two parton shower background for associate W Higgs production

---

**E. Levin<sup>\*</sup> and J. Miller<sup>†</sup>**

*Department of Particle Physics, School of Physics and Astronomy  
Raymond and Beverly Sackler Faculty of Exact Science  
Tel Aviv University, Tel Aviv, 69978, Israel*

**ABSTRACT:** The estimates of the background for the associate W Higgs production, which stems from the two parton shower production. It is about  $1 \div 2.5$  times larger than the signal. However, this background does not depend on the rapidity difference between the W and the  $b\bar{b}$  pair, while the signal peaks when the rapidity difference is zero. The detailed calculations for the enhanced diagrams' contribution to this process, are presented, and it is shown that the overlapping singularities, being important theoretically, lead to a negligible contribution for the LHC range of energies.

**KEYWORDS:** Higgs production, BFKL Pomeron, Pomeron loops, correlation function, overlapping singularities, W inclusive production, W and quark -antiquark associate production.

---

<sup>\*</sup>Email: leving@post.tau.ac.il, levin@mail.desy.de;

<sup>†</sup>Email: jeremymiller@london.com, jeremymi@post.tau.ac.il;

---

## Contents

|   |           |
|---|-----------|
| <b>1. Introduction</b>  | <b>1</b>  |
| <b>2. One parton shower contribution: one BFKL Pomeron exchange and inclusive cross section</b>                 | <b>3</b>  |
| <b>3. Two parton shower contribution to the background for W boson and Higgs production</b>                     | <b>10</b> |
| 3.1 The simplest diagram  | 10        |
| 3.2 The two parton shower production: enhanced diagram  | 12        |
| 3.2.1 Region (I): $ i\nu + 1/2  \ll \nu_1 + \nu_2$ ( $ i\nu' + 1/2  \ll \nu'_1 + \nu'_2$ )                      | 17        |
| 3.2.2 Region (II): $ i\nu + 1/2  \gg \nu_1 + \nu_2$ ( $ i\nu' + 1/2  \gg \nu'_1 + \nu'_2$ )                     | 17        |
| 3.2.3 Region (III): $ i\nu + 1/2  \approx \nu_1 + \nu_2$ ( $ i\nu' + 1/2  \approx \nu'_1 + \nu'_2$ )            | 21        |
| 3.2.4 Region (IV): $\nu \ll 1, \nu_1 \ll 1$ and $\nu_2 \ll 1$ ( $\nu' \ll 1, \nu'_1 \ll 1$ and $\nu'_2 \ll 1$ ) | 23        |
| <b>4. Estimates of the background</b>   | <b>25</b> |
| <b>5. Summary</b>   | <b>27</b> |
| <b>A. Appendix</b>  | <b>28</b> |
| A.1 The amplitude for the subprocess in $GG \rightarrow W$  | 28        |
| A.2 The amplitude for subprocess $GG \rightarrow b\bar{b}$  | 31        |
| A.3 The amplitude for the inclusive Higgs production via subprocess $GG \rightarrow H$                          | 33        |

---

## 1. Introduction

The most important discovery, that everybody expects at the LHC, is the discovery of the Higgs boson. The exclusive process which has the best experimental signature, as far as we know, is diffractive Higgs production. Having two large rapidity gaps between the Higgs and the recoiled protons, this process has a minimal background from QCD processes without the Higgs. However, the total cross section for diffractive Higgs production turns out to be very small, namely about 3 fb (see detailed estimates by the Durham group, in Ref. [1]). The largest cross section out of all the different processes for Higgs production, is the cross section for inclusive Higgs production, which reaches 40 - 50 pb (assuming that the Higgs mass  $M_H \approx 100 \text{ GeV}/c^2$ ).

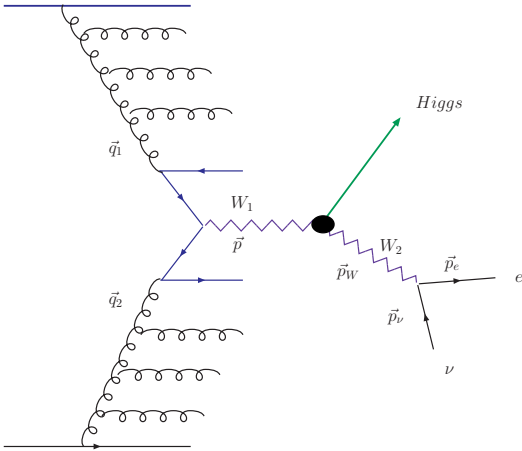


**Figure 1:** The associate W boson and Higgs production.

Unfortunately, the background for this process turns out to be so large, that any experimental measurement of the Higgs in an inclusive process, looks rather problematic. In his talk at GGI WS (Florence 2007), Hannes Jung made the suggestion of measuring the associate Higgs production, which is the inclusive production of the Higgs together with the W boson. This process has a cross section which is about 1.5% of that of the cross section for inclusive Higgs production, but this smallness could be compensated by its improved experimental signature. This process yields the production of the W boson and the Higgs, at more or less the same rapidity values (see Fig. 1). The value for the cross section for this process, can be found only to within an accuracy of 30%, due to

large uncertainties in the values of the structure functions. However, the ratio

$$R_1 = \frac{\sigma(pp \rightarrow WH + X)}{\sigma(pp \rightarrow W + X)} \approx 3.5 \times 10^{-8} \quad (1.1)$$

is known to within 7% accuracy. In this paper, we estimate the cross section of the main background process, namely, the associate production of the W boson and the  $b\bar{b}$  pair, which has a mass close to  $M_H$ , and is produced at more or less the same value of rapidity. It is easy to see, that if we assume that the W boson and the  $b\bar{b}$  pair are produced independently of the different parton showers, the ratio of the signal to the background can be estimated using the following equation

$$R = \frac{\sigma(pp \rightarrow WH + X)}{\sigma(pp \rightarrow W + [b\bar{b}] + X)} \approx \frac{R_1}{\frac{\sigma(pp \rightarrow [b\bar{b}] + X)}{\sigma_{tot}}}$$

This simple estimate for the cross section for  $b\bar{b}$  production, gives

$$\sigma(pp \rightarrow [b\bar{b}] + X) \propto \frac{\alpha_S^2(M_H)}{M_H^2} \quad (1.2)$$

and, using  $\sigma_{tot} = 110 \text{ mb}$  (see Ref. [2]), we obtain

$$R \sim 9 \div 10 \quad (1.3)$$

However, we see two sources for an increase of the  $b\bar{b}$  production cross section. These are the energy growth of the cross section due to the gluon structure function, and the positive correlation between the

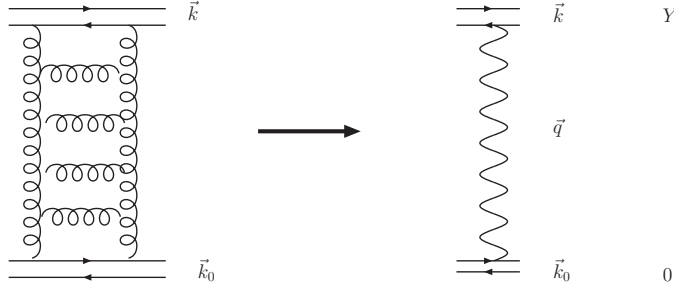


**Figure 2:** The exchange of the single BFKL Pomeron.

W boson and the  $b\bar{b}$  production, which has been seen at the Tevatron [3]. The estimates of both sources, are the subject of this paper.

This paper is organized as follows. In the next section, we calculate the cross sections for inclusive W boson and  $b\bar{b}$  production, with a particular focus on the energy dependence of the cross section.

The main section of this paper is the third, where we consider the correlation function for inclusive W boson and  $b\bar{b}$  production. We show that this correlation function can be reduced to the calculation of the specific enhanced diagrams, for the BFKL Pomeron interaction. The detailed calculations of the enhanced diagrams are presented in this section, which include the integration over the entire kinematic region. In particular, the overlapping singularities are taken into account. Calculating this diagram, and comparing this calculation with the experimental data obtained at the Tevatron, we will be able to provide a reliable estimate in section 4 of the ratio of Eq. (1.2), at the LHC range of energies. In the conclusion we summarise our results.

## 2. One parton shower contribution: one BFKL Pomeron exchange and inclusive cross section

In this section, we will discuss the calculation of the inclusive cross section. Due to the factorisation theorem [4, 5], and the AGK cutting rules [6], only the production from one parton shower contributes to the single inclusive cross section. We begin with a discussion of the one BFKL Pomeron exchange amplitude.

In the calculations that follow, let  $\vec{k}_i$  denote the momenta conjugate to the size of the interacting dipoles.  $\vec{q}_i$  are the momenta transferred along the Pomerons. The diagram of Fig. 2 shows the scattering of the dipole with rapidity  $Y$ , and transverse momentum  $\vec{k}$ , off the dipole at rapidity  $Y = 0$ , which carries transverse momentum  $\vec{k}_0$ , due to the exchange of one Pomeron. In this notation, the amplitude of Fig. 2 has the expression[7]

$$A(1P) = \sum_{n=-\infty}^{+\infty} \oint_C d\gamma g(\vec{k}, \vec{q}; \gamma_n) e^{\omega(\gamma_n)(Y-Y')} h(\gamma_n) g(\vec{k}_0, \vec{q}; \tilde{\gamma})$$

where  $h(\gamma_n) = \left(\gamma_n - \frac{1}{2}\right)^2 \lambda(\gamma_n)$  and  $\lambda(\gamma_n) = (\gamma_n(1 - \gamma_n))^{-2}$  (2.1)

where the conformal variable  $\gamma_n$ , is defined in Eq. (2.2) as

$$\gamma_n = \frac{1+n}{2} + i\nu \quad \tilde{\gamma}_n = 1 - \gamma_n^* = \frac{1-n}{2} + i\nu \quad (2.2)$$

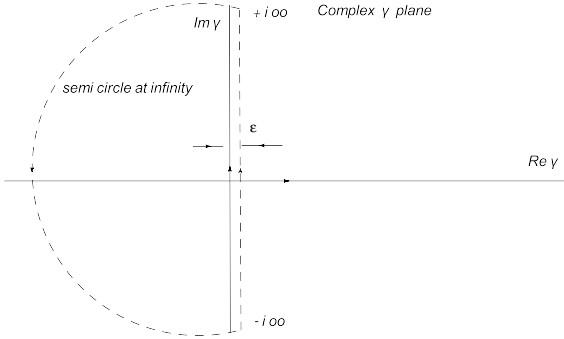


**Figure 3:** Contour enclosing singularities for integration over the conformal variable  $\gamma$ .

The contour  $C$  consists of the imaginary  $\gamma$  axis from  $\pm i\infty$ , and the semi circle at  $\infty$ , to the left of the imaginary  $\gamma$  axis, which encloses all singularities in the integrand of Eq. (2.1) (see Fig. 3). Since  $g(\vec{k}, \vec{q}; \gamma) g(\vec{k}_0, \vec{q}; \tilde{\gamma}) \propto (k^2/k_0^2)^\gamma$  for  $k^2 > k_0^2$ , the integrand vanishes on the semi circle at  $\pm i\infty$ , such that it is sufficient just to replace

$$\oint_C d\gamma_n \rightarrow \int_{\epsilon-i\infty}^{\epsilon+i\infty} d\gamma_n \quad (2.3)$$

In evaluating the integral of Eq. (2.1), and in particular for the first enhanced diagram, the calculations that follow will be more economical if the integrals are expressed in terms of the variable  $\nu$ , instead of the variable  $\gamma_n$ , (where the relationship between  $\gamma_n$  and  $\nu$  is given in Eq. (2.2)). For the integration limits  $\epsilon + i\infty \leq \gamma \leq \epsilon + i\infty$  (as  $\epsilon \rightarrow 0$ ), then Eq. (2.2) gives the corresponding limits of integration for the variable  $\nu$  as  $-\infty \leq \nu \leq \infty$ , and one should sum over all real positive integers  $n$  in Eq. (2.2). In this way in Eq. (2.1), one can replace the integration over  $\gamma_n$  with the integration over  $\nu$  using the notation

$$\sum_{n=-\infty}^{\infty} \int_{\epsilon-i\infty}^{\epsilon+i\infty} d\gamma_n = \sum_{n=-\infty}^{\infty} \int_{-\infty}^{\infty} d\nu \quad (2.4)$$

The notation  $\sum_{n=-\infty}^{\infty} \int_{-\infty}^{\infty} d\nu$ , corresponds to the integration over the quantum numbers associated with the continuous unitary variable irreducible representations of  $SL(2, C)$ , defined in Eq. (2.2). The energy levels are the  $SL(2, C)$  eigenvalues of the BFKL kernel, given by

$$\omega(\gamma_n) = \bar{\alpha}_S \{ \psi(1) - \Re(\psi(\gamma_n)) \} = \bar{\alpha}_S \{ 2\psi(1) - \psi(\gamma_n) - \psi(1 - \gamma_n) \} \quad (2.5)$$

$$= \bar{\alpha}_S \left\{ \psi(1) - \operatorname{Re} \psi \left( \frac{|n|+1}{2} + i\nu \right) \right\} \quad (2.6)$$

where  $\psi(f) = d/df (\ln \Gamma(f))$ , and  $g(\vec{k}, \vec{q}; \gamma_n)$ , are the eigenfunctions. Thus, the one BFKL pomeron exchange amplitude shown in Fig. 2, has this expression in  $\nu$  notation

$$\begin{aligned} A(1P) &= \int_{-\infty}^{\infty} d\nu g_P(\vec{k}, \vec{q}; n=0, \nu) e^{\omega(n=0, \nu)(Y-Y')} \nu^2 \lambda(n=0, \nu) g_P(\vec{k}_0, \vec{q}; n=0, -\nu) \\ &= \int_{-\infty}^{\infty} d\nu g_P(\vec{k}, \vec{q}; \nu) e^{\omega(\nu)(Y-Y')} \nu^2 \lambda(0, \nu) g_P(\vec{k}_0, \vec{q}; -\nu) \end{aligned} \quad (2.7)$$

where in terms of  $\nu$

$$\lambda(n, \nu) = \frac{1}{[\frac{(n+1)^2}{4} + \nu^2][\frac{(n-1)^2}{4} + \nu^2]} \quad (2.8)$$

In Eq. (2.7), it is assumed that  $n=0$ , in order to find the largest contribution at high energy. From now onwards, the notation  $\omega(\nu) = \omega(n=0, \nu)$  will be used (see Eq. (2.6)), and  $\lambda(\nu) = \lambda(n=0, \nu)$  and  $g(\vec{k}, \vec{q}; \nu) = g(\vec{k}, \vec{q}; n=0, \nu)$ . In Eq. (2.7),  $g_P(q, k; n=0, \nu) = \Gamma_P(k, q) g(q, k; n=0, \nu)$  and  $g(q, k; n=0, \nu)$  has been calculated in Ref.[8], which takes the form

$$g(k, q; \nu) = \frac{(q\bar{q})^{i\nu}}{|k|} \left\{ C_1(\nu) \left( \frac{q^2}{16k^2} \right)^{-i\nu} F(\nu) - C_2(\nu) \left( \frac{q^2}{16k^2} \right)^{i\nu} F(-\nu) \right\} \quad (2.9)$$

$$\text{where } F(\nu) = {}_2F_1 \left( \frac{1}{4} - \frac{1}{2}i\nu, \frac{3}{4} - \frac{1}{2}i\nu, 1 - i\nu, \frac{q^2}{4k^2} \right) {}_2F_1 \left( \frac{1}{4} - \frac{1}{2}i\nu, \frac{3}{4} - \frac{1}{2}i\nu, 1 - i\nu, \frac{(q^*)^2}{4(k^*)^2} \right)$$

$$\text{and where } C_1(\nu) = \frac{2^{-2i\nu} \pi^2}{-i\nu} \frac{\Gamma^2(\frac{1}{2} - i\nu) \Gamma(i\nu)}{\Gamma^2(\frac{1}{2} + i\nu) \Gamma(-i\nu)} \quad C_2(\nu) = \frac{2^{-2i\nu} \pi^2}{-i\nu} \frac{\Gamma^2(1 - i\nu) \Gamma(i\nu)}{\Gamma^2(1 + i\nu) \Gamma(-i\nu)} \quad (2.10)$$

From this definition, one notes the following interesting property of  $C_1(\nu)$ , namely

$$C_1(\nu) C_1(-\nu) = \frac{\pi^4}{\nu^2} \quad (2.11)$$

In the limit that  $q \ll k$ , then the function  $F(\nu)$  defined in Eq. (2.10) tends to unity, and Eq. (2.9) reduces to

$$g(k, q, n=0, \nu) = \frac{C_1(\nu)}{|k|} (16k^2)^{i\nu} \quad (2.12)$$

$\Gamma_P(k, q)$  is the so called impact factor, which is equal to

$$\Gamma_P(k, q) = \sum_i \int \prod_i d^2x_i d^2y_i |\Psi(\{x_i, y_i\})|^2 e^{\vec{q} \cdot \frac{1}{2}(\vec{x}_i - \vec{y}_i)} \left( 1 - e^{\vec{k} \cdot (\vec{x}_i - \vec{y}_i)} \right) \quad (2.13)$$

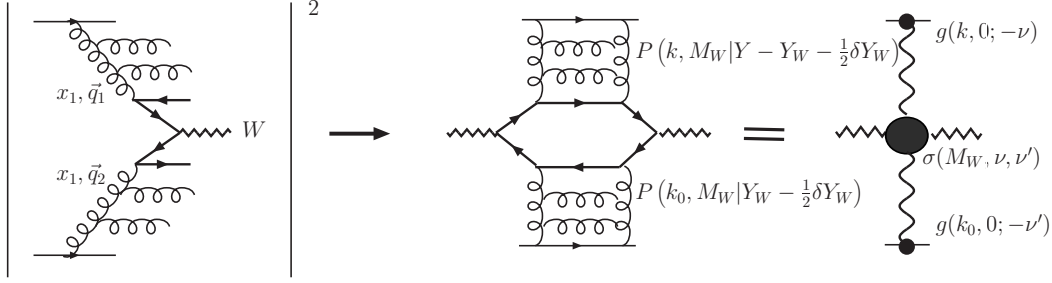


**Figure 4:** The inclusive production in the BFKL Pomeron approach.

where  $\Psi(\{x_i, y_i\})$  is the wave function of the proton written in terms of the colourless dipoles, where  $x_i$  and  $y_i$  are the coordinates of the dipole  $i$  (here  $|\vec{x}_i - \vec{y}_i|$  is the dipole size). It is convenient to calculate the amplitude for single pomeron exchange of Eq. (2.7), for the case of  $\vec{q} = 0$ , since we are considering here the contribution of the BFKL Pomeron to the total cross section. Hence, assuming that  $k_0^2 \ll k^2$ , and using the expression of Eq. (2.9) for  $g(q, k; n = 0, \nu)$

$$A(1P) = \frac{\pi^4}{(k^2 k_0^2)^{1/2}} \Gamma_P(k, q = 0) \Gamma_P(k_0, q = 0) P(k; k_0 | Y - Y')$$

where  $P(k; k_0 | Y - Y') = \int_{-\infty}^{\infty} \frac{d\nu}{2\pi i} e^{\omega(\nu)(Y - Y')} \lambda(0, \nu) \left(\frac{k^2}{k_0^2}\right)^{i\nu}$  (2.14)

It should be noted that  $P(k; k_0 | Y - Y')$  is the dimensionless amplitude for the single BFKL pomeron exchange, where as  $A(1P)$  is related to the cross section, and it has the dimensions of  $\text{GeV}^{-2}$ . The integration over  $\nu$  can be evaluated by expanding the BFKL function  $\omega(\nu)$ , around the saddle point  $\nu = 0$  (see Eq. (2.6))

$$\omega(\nu) = \omega(0) - \frac{1}{2} \nu^2 \omega''(0) \quad (2.15)$$

Then the integration over  $\nu$  in Eq. (2.14), reduces to a Gaussian integral, and evaluating the  $\nu$  integration, gives the expression for single Pomeron exchange as the expression

$$[A(1P)]_{\nu \rightarrow 0} = \frac{\pi^4 \Gamma_P(k, q = 0) \Gamma_P(k_0, q = 0)}{(k_0^2 k^2)^{\frac{1}{2}}} P(k; k_0 | Y - Y') \quad (2.16)$$

where  $P(k; k_0 | Y - Y') = e^{\omega(0)Y} \left(\frac{2\pi}{\omega''(0)Y}\right)^{\frac{1}{2}}$  (2.17)

It should be stressed, that the value of  $\nu$  in this integral is small, namely ( $\nu = \ln(k^2/k_0^2)/(\omega''(0)Y) \ll 1$ ), justifying our expansion in Eq. (2.15). It should be noted, that in Eq. (2.14), contains as the initial condition at  $Y - Y' = 0$ , the exchange of two gluons in the Born Approximation of perturbative QCD. Indeed, in this case, the contour in  $\nu$  can be closed on the singularities of  $\lambda(n = 0, \nu)$ , which are the poles of the second order at  $\nu = \pm i\frac{1}{2}$ . Considering the case when  $k^2 > k_0^2$ , we close the contour on the point  $\nu = +\frac{1}{2}i$ , and obtain the following expression

$$P(k; k_0 | Y - Y' \rightarrow 0) \longrightarrow \sqrt{\frac{k_0^2}{k^2}} \ln(k^2/k_0^2) \quad (2.18)$$

which leads to

$$A(1P) = \frac{\pi^4 \Gamma_P(k, q=0) \Gamma_P(k_0, q=0)}{k^2} \ln(k^2/k_0^2) \quad (2.19)$$

Eq. (2.19) is the answer for the Born approximation of perturbative QCD, (namely, for the case of two gluon exchange). For the case of calculating the inclusive cross section, we can use the  $k_t$  factorisation theorem [4, 5], using the Mueller technique [9], which allows one to reduce the calculation of the inclusive cross section to the case of single Pomeron exchange, using the optical theorem (see Fig. 4, where the inclusive production of the W boson is shown in the Mueller technique [9]). Indeed, according to the factorisation theorem, the inclusive production can be written as [10]

$$\frac{d\sigma}{dY_W} = \int dx_1 dx_2 \int d^2 q_1 d^2 q_2 \phi(x_1, q_1) \phi(x_2, q_2) \sigma(M_W, q_1, q_2) \delta(x_1 x_2 s - M_W^2) \quad (2.20)$$

where  $s$  is the energy of the collision, and  $\phi(x_i, q_i)$  is the un-integrated structure function, which is related to the gluon structure function in the following way

$$x_i G(x_i, q^2) = \int^{q^2} dk^2 \phi(x_i, k^2) \quad (2.21)$$

where the  $x_i$  are equal to

$$x_1 = \frac{M_W}{\sqrt{s}} e^{Y_W} ; \quad x_2 = \frac{M_W}{\sqrt{s}} e^{-Y_W} ; \quad (2.22)$$

where  $Y_W$  is the rapidity of the W boson in the center of mass frame (c.m.f.). The un-integrated structure function at high energy can be rewritten through the Pomeron exchange, while the hard cross section in Eq. (2.20) is calculated in the appendix. The integrals over  $q_1$  and  $q_2$  in Eq. (2.20), are convergent at  $q_1 \approx M_W$  and  $q_2 \approx M_W$ , and because of this, one can rewrite Eq. (2.20) in a simpler form, namely



$$\frac{d\sigma_{incl} \left( \ln \left( s/M_{b,\bar{b}}^2 \right); Y_{b\bar{b}}; 0 \right)}{dy_{b\bar{b}}} = \quad (2.23)$$

$$\sigma(M_{b\bar{b}}) \Gamma_P(k, q=0) \Gamma_P(k_0, q=0) \sqrt{\frac{M_{b\bar{b}}^4}{k^2 k_0^2}} P \left( k, M_{b,\bar{b}} | Y - Y_{b\bar{b}} - \frac{1}{2} \delta Y_{b\bar{b}} \right) P \left( k_0, M_{b,\bar{b}} | Y_{b\bar{b}} - \frac{1}{2} \delta Y_{b\bar{b}} \right) \\ \frac{d\sigma_{incl} \left( \ln \left( s/M_W^2 \right); Y_W; 0 \right)}{dY_W} = \quad (2.24)$$

$$\sigma(M_W) \Gamma_P(k, q=0) \Gamma_P(k_0, q=0) \sqrt{\frac{M_W^4}{k^2 k_0^2}} P \left( k, M_W | Y - Y_W - \frac{1}{2} \delta Y_W \right) P \left( k_0, M_W | Y_W - \frac{1}{2} \delta Y_W \right)$$

In Eq. (2.24),  $\sigma(M_W)$  is the squared amplitude of the quark hexagon contribution shown in Fig. 5, and  $\sigma(M_{b\bar{b}})$  is the squared amplitude of the quark subprocess contribution shown in Fig. 6. Both have the dimensions of cross section, namely  $\sigma(M_W)$  and  $\sigma(M_{b\bar{b}})$  have dimensions of  $\text{GeV}^{-2}$  (see Eq. (2.27) and Eq. (2.29) respectively).  $Y = \ln(s/m^2)$ , and  $Y_W$  and  $Y_{b\bar{b}}$  are respectively the rapidity values in the laboratory frame of the W boson, and the center of mass of the quark anti-quark pair.  $\delta Y_W \equiv \ln(M_W^2/m^2)$  and  $\delta Y_{b\bar{b}} \equiv \ln(M_{b\bar{b}}^2/m^2)$  are the rapidity windows occupied by the W boson and the  $[b\bar{b}]$  pair, respectively. The arguments in the single Pomeron amplitudes in Eq. (2.24), follow directly from Eq. (2.22). For  $P$ , we can use Eq. (2.14), for example

$$P \left( k, M_W | Y - Y_W - \frac{1}{2} \delta Y_W \right) = \int_{-\infty}^{\infty} \frac{d\nu}{2\pi i} e^{\omega(\nu)(Y - Y_W - \frac{1}{2} \delta Y_W)} \left( \frac{M_W^2}{k^2} \right)^{i\nu} \quad (2.25)$$

Using Eq. (2.18), one can see that at low energies,  $Y \rightarrow \delta Y_W$ , and Eq. (2.24) reduces to the expression

$$\frac{d\sigma_{incl} \left( \ln \left( s/M_W^2 \right); Y_W; 0 \right)}{dY_W} \longrightarrow \Gamma_P(k, q=0) \Gamma_P(k_0, q=0) \ln(M_W^2/k^2) \ln(M_W^2/k_0^2) \sigma(M_W) \quad (2.26)$$

which is exactly the same as the expression for the cross section in the Born approximation of perturbative QCD, ( see Eq. (2.28)), with  $k^2 = k_0^2 = q_{\perp, \min}^2$ , and  $\Gamma_P(k, q=0) = \bar{\alpha}_S(k^2)$ . It is easy to see, that Eq. (2.23) has the form of Eq. (2.30), in the low energy limit.

The Mueller diagram in the Born approximation of pQCD for the inclusive W boson production, is shown in Fig. 4, and the formula for this cross section is given by Eq. (2.24). We need only to calculate  $\sigma(M_W)$  and  $\sigma(M_{b\bar{b}})$ . The easiest way to derive these cross sections, is to calculate them in the Born approximation of perturbative QCD ( see Fig. 5 and Fig. 6). The calculations of the expressions for the cross sections for the processes of Fig. 5 and Fig. 6, are presented in appendices A-3 and A-4, and the final expressions for the amplitudes of these diagrams take the form

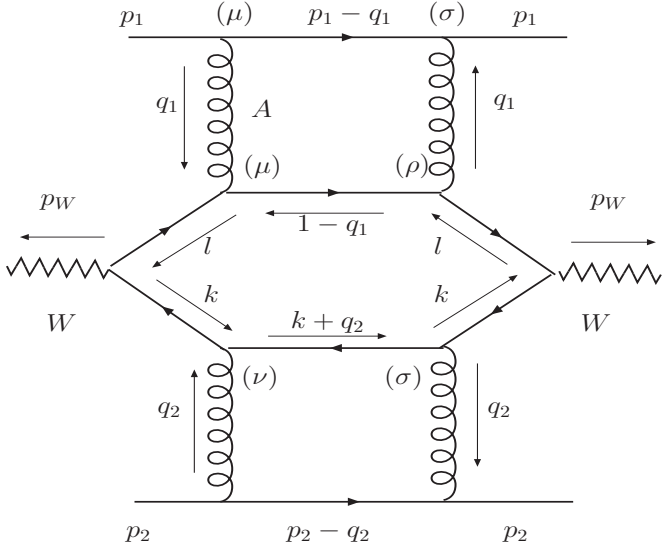


**Figure 5:** Born Approximation for W boson inclusive production.

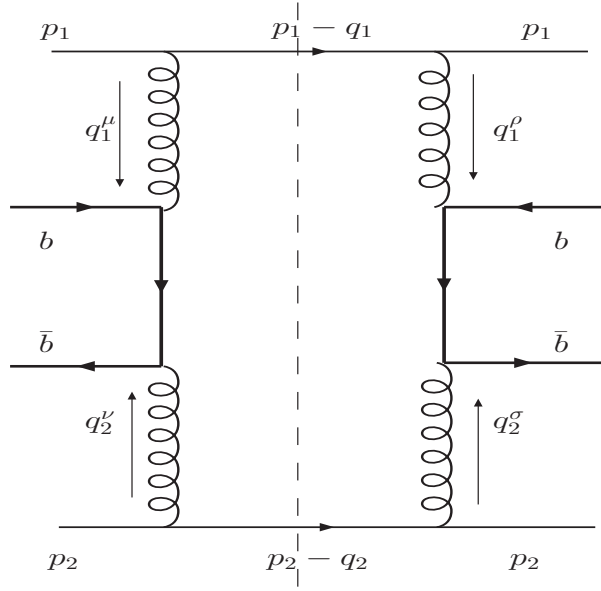


**Figure 6:** Born Approximation for quark anti-quark inclusive production.

- for  $\sigma(M_W, q_1, q_2)$  (see Fig. 5 and Eq. (A.1.13))

$$\sigma(M_W, q_1, q_2) = \frac{\alpha_S^2(q^2)}{q_{1,\perp}^2 q_{2,\perp}^2} \sigma(M_W)$$

where

$$\sigma(M_W) = \left( \frac{N_c^2 - 1}{2N_c} \right)^2 \frac{1}{4N_c} \frac{\alpha_S^2}{4\pi^3} \sqrt{2} G_F \ln \left( \frac{M_W^2}{4m_u^2} \right) \ln \left( \frac{M_W^2}{4m_d^2} \right) \quad (2.27)$$

Recall that the Fermi coupling  $G_F$  has the dimensions of  $\text{GeV}^{-2}$ , so that inspection of Eq. (2.27), shows that  $\sigma(M_W)$  has the dimensions of the cross section. The factor in front of  $\sigma(M_W)$ , (in the first line of Eq. (2.27)), is taken into account in the BFKL Pomeron exchange in Eq. (2.24). Integrating over the transverse momenta  $\vec{q}_{1,\perp}$  and  $\vec{q}_{2,\perp}$  on the RHS of Eq. (2.27), one obtains the following expression for the Born amplitude of Fig. 5.

$$\sigma(M_W, q_1, q_2) = \alpha_S^2(q^2) \pi^2 \ln^2 \left( \frac{M_W^2}{q_{\perp,\min}^2} \right) \sigma(M_W) \quad (2.28)$$

- for  $\sigma(M_{b\bar{b}}, q_1, q_2)$  (see Fig. 6 and Eq. (A.2.7))

$$\sigma(M_{b\bar{b}}, q_1, q_2) = \frac{\alpha_S^2(q^2)}{q_{1,\perp}^2 q_{2,\perp}^2} \sigma(M_{b\bar{b}})$$

where

$$\sigma(M_{b\bar{b}}) = \left( \frac{N_c^2 - 1}{2N_c} \right)^2 \frac{1}{4N_c} \frac{\alpha_S^2}{8\pi} \frac{1}{M_{b\bar{b}}^2} \ln \left( \frac{M_W^2}{4m_b^2} \right) \quad (2.29)$$

Integrating over the transverse momenta  $\vec{q}_{1,\perp}$  and  $\vec{q}_{2,\perp}$  on the RHS of Eq. (2.29), one obtains the following expression for the Born amplitude of Fig. 6.

$$\sigma(M_{b\bar{b}}, q_1, q_2) = \alpha_S^2(q^2) \pi^2 \ln^2 \left( \frac{M_{b\bar{b}}^2}{q_{\perp,\min}^2} \right) \sigma(M_{b\bar{b}}) \quad (2.30)$$

### 3. Two parton shower contribution to the background for W boson and Higgs production

#### 3.1 The simplest diagram

For the associate W boson and Higgs production, we expect a small background, since the main process which creates such a background, namely,

$$p + p \rightarrow b\bar{b} + W + X \quad (3.1.1)$$

leads to a negligible contribution if both the  $W$  and the  $b\bar{b}$  pair are produced from one parton shower, at  $Y_{b\bar{b}} \approx Y_W$ . Here,  $Y_{b\bar{b}}$  is the value for the rapidity of the quark anti-quark pair, namely,  $Y_{b\bar{b}} = \frac{1}{2}(Y_b + Y_{\bar{b}})$  and  $Y_W$  is the Higgs boson rapidity. Indeed, in one parton shower, the typical difference ( $\Delta y$ ) in the rapidity between the two emitted partons, are larger (or equal to)  $1/\alpha_S \gg 1$ . Therefore, keeping  $|Y_{b\bar{b}} - Y_W| \leq 1/\alpha_S$ , we have a suppression for the production of the W boson and the quark anti-quark pair.

However, there exists a process for the production of the quark anti-quark pair and W boson production, from two different parton showers (see Fig. 7). In this process, we do not expect any suppression of the quark anti-quark pair, and W boson production, at the same values of rapidity. However, this has its own suppression, which is related to the small probability associated with having two parton shower processes. However, at high energies, this suppression is not actually very strong, as we will demonstrate below.

The general expression for the diagram of Fig. 7 has the following form

$$A(\text{Fig. 7}) = \int \frac{d^2q}{(2\pi)^2} V^2(pp \rightarrow lPl; \vec{q}) \frac{d\sigma_{incl}(\ln(s/M_{b,\bar{b}}^2); Y_{b\bar{b}}; -\vec{q})}{dY_{b\bar{b}}} \frac{d\sigma_{incl}(\ln(s/M_W^2); Y_W; -\vec{q})}{dY_W} \quad (3.1.2)$$

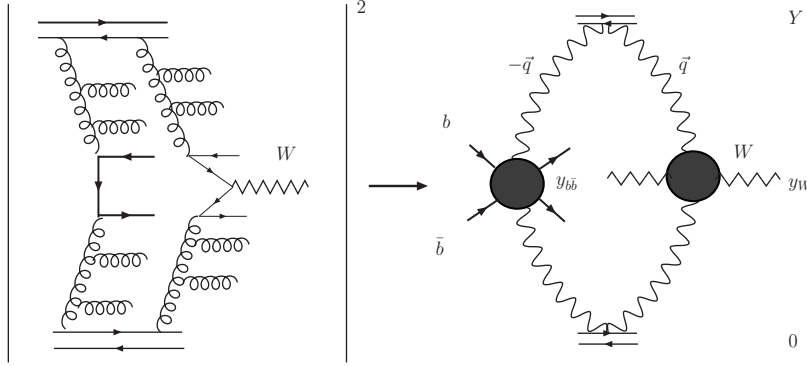


**Figure 7:** The simplest Mueller diagram for the two parton shower contribution to the background for the W boson and Higgs production

$V(pp \rightarrow \mathbb{P}\mathbb{P})$  in Eq. (3.1.2) and Eq. (3.1.3) below is the vertex of the interaction of the two Pomerons with the proton (see Fig. 7). In Eq. (3.1.2),  $d\sigma_{incl}/dy$  is the cross section for the inclusive production of the W boson, and/or the quark anti-quark pair, but not at  $q = 0$ . However, at high energy and for hard processes, we can assume that the value of the typical  $q$  is small, and it is of the order of the typical momenta inside of the proton. At high energy, the mechanism for inclusive production is related to the emission of one parton shower, which can be described by the DGLAP evolution [11], or by the BFKL Pomeron exchange [7]. For both cases, it has been proved [12, 13, 8] that we can safely put  $q = 0$  in our evaluation of the integral of Eq. (3.1.2). Therefore,

$$\begin{aligned}
 A(Fig. 7) &= \frac{d\sigma_{incl}(\ln(s/M_{b,\bar{b}}^2); Y_{b\bar{b}}; 0)}{dY_{b\bar{b}}} \frac{d\sigma_{incl}(\ln(s/M_W^2); Y_W; 0)}{Y_W} \times \int \frac{d^2q}{(2\pi)^2} V^2(pp \rightarrow \mathbb{P}\mathbb{P}; \vec{q}) \\
 &= \frac{\frac{d\sigma_{incl}(\ln(s/M_{b,\bar{b}}^2); Y_{b\bar{b}}; 0)}{dY_{b\bar{b}}}}{2\sigma_{eff}} \frac{\frac{d\sigma_{incl}(\ln(s/M_W^2); Y_W; 0)}{dY_W}}{Y_W}
 \end{aligned} \tag{3.1.3}$$

Fortunately for us, the value of  $\sigma_{eff}$  has been measured by the CDF collaboration at the Tevatron [3], with the result  $\sigma_{eff} = 14.5 \pm 1.7 \pm 2.3$  mb. Using the value of the predicted cross section for  $b\bar{b}$  production, taking  $M_{b\bar{b}} = M_H = 100$  GeV/c<sup>2</sup> [15] for  $Y_{b\bar{b}} = 0$ , and at the LHC energy, namely,  $\frac{d\sigma_{incl}(\ln(s/M_{b,\bar{b}}^2); Y_{b\bar{b}}; 0)}{dY_{b\bar{b}}} = 2 \times 10^{-6}$  mb\*, one can obtain from Eq. (3.1.3) (comparing it with Eq. (1.1)), that

$$\frac{d\sigma_{background}(Eq. (3.1.3))/dy_{b\bar{b}}|_{Y_{b\bar{b}}=0}}{d\sigma_{H \text{ production}}/dY_H|_{Y_H=0}} \approx 2 \quad \text{in the LHC energy range} \tag{3.1.4}$$

---

\*This value, together with a more detailed consideration of the value of the cross section for  $b\bar{b}$  inclusive production, will be discussed in section 4

This ratio can be easily reduced using the characteristic property of the process of Fig. 7, namely that there are no correlations in the rapidity values between the  $W$  boson, and the quark anti-quark pair. In other words, the cross section for this process does not depend on the difference  $Y_W - Y_{b\bar{b}}$ , while the cross section for the associate  $W$  Higgs production of Fig. 1, has a maximum at  $Y_W - Y_{b\bar{b}} = 0$ .

This result is encouraging, but we need to estimate the more complicated diagrams to derive the final conclusions (see Fig. 8).

### 3.2 The two parton shower production: enhanced diagram

In the diagram of Fig. 8, the two parton showers are produced at the rapidity  $y_1$ , and they merge back to one parton shower at the rapidity  $y_2$ . Such a process can be reduced to the enhanced BFKL Pomeron diagram at high energy, as it is shown in Fig. 8. We would like to recall, that in this simplification, we use the unitarity constraint

$$2\text{Im } A_{el} = |A_{el}|^2 + G_{in} \quad (3.2.1)$$

where  $A_{el}$  is the elastic scattering amplitude at energy  $s$  and impact parameter  $b$ , while  $G_{in}$  is the contribution of all inelastic processes. The scattering amplitude is purely imaginary at high energy, and it can be described by the exchange of one BFKL Pomeron. Neglecting  $|A_{el}|$  in Eq. (3.2.1), which is possible for the range of energies  $\alpha_S \ln(s/s_0) \ll \ln(1/\alpha_S^2)$ , we obtain from Eq. (3.2.1) the relation

$$2 A(1P) = G_{in}(s, b) \quad (3.2.2)$$

where  $A(1P)$  is the amplitude for one BFKL Pomeron exchange. Using this relation, we are able to replace the production of the parton showers with the exchange of the BFKL Pomerons. In this subsection, we will calculate the simplest enhanced diagram shown in Fig. 8, whose contribution is given by the expression

$$\begin{aligned} A(P \rightarrow 2P \rightarrow P; Fig. 8) &= \oint_C h(\gamma) d\gamma \prod_{i=1}^2 \oint_{C_i} h(\gamma_i) d\gamma_i \oint_{C'_i} h(\gamma'_i) d\gamma'_i \oint_{C'} h(\gamma') d\gamma' \\ &\times \int_{Y_W + \frac{1}{2}\delta Y_W}^Y dY_1 \int_0^{Y_{b\bar{b}} - \frac{1}{2}\delta Y_{b\bar{b}}} dY_2 g_P(\vec{k}, \vec{q} = 0; -\gamma) \lambda^{-1}(\gamma) e^{\omega(\gamma)(Y-Y_1)} e^{\omega(\gamma_1)(Y_1-Y_W - \frac{1}{2}\delta Y_W)} \\ &\times e^{\omega(\gamma_2)(Y_1-Y_{b\bar{b}} - \frac{1}{2}\delta Y_{b\bar{b}})} e^{\omega(\gamma'_1)(Y_W - \frac{1}{2}\delta Y_W - Y_2)} e^{\omega(\gamma'_2)(Y_{b\bar{b}} - \frac{1}{2}\delta Y_{b\bar{b}} - Y_2)} e^{\omega(\gamma')(Y_2-0)} \\ &\times g_P(\vec{k}_0, \vec{q} = 0; \gamma') \lambda^{-1}(\gamma') \sigma(M_W, -\gamma_1, \gamma'_1) \sigma(M_{b\bar{b}}, -\gamma_2, \gamma'_2) \\ &\times \int d^2 q' \Gamma_{3P}(\vec{q} = 0, -\vec{q}'|\gamma, \gamma_1, \gamma_2) \Gamma_{3P}(\vec{q} = 0, -\vec{q}'|-\gamma', -\gamma'_1, -\gamma'_2) \end{aligned} \quad (3.2.3)$$

where  $h(\gamma)$  and  $\lambda(\gamma) = (\gamma(\gamma-1))^{-2}$  have been defined in Eq. (2.1). The contours  $C, C', C_1, C_2, C'_1$  and  $C'_2$  are similar to the contour shown in Fig. 3, which consists of the imaginary  $\gamma$  axis from

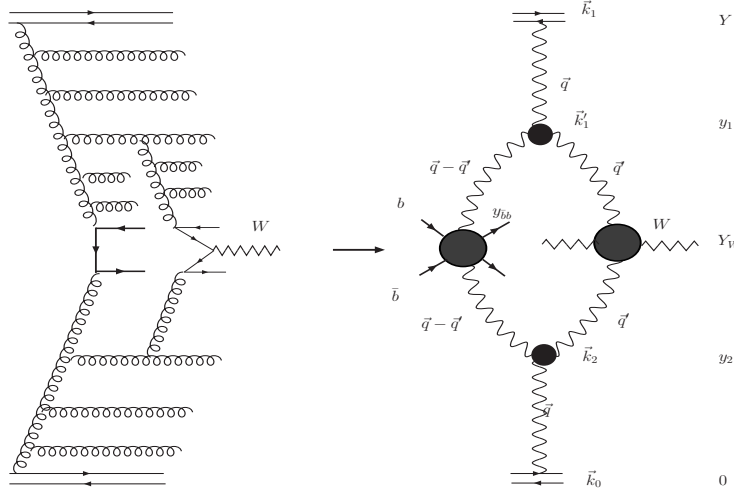


**Figure 8:** The first enhanced Mueller diagram for two parton shower contribution to the background for the  $W$  boson and Higgs production

$\pm i\infty$ , and the semi circle at  $\infty$  to the left of the imaginary  $\gamma$  axis, which encloses all singularities in the integrand of Eq. (3.2.3). In this case also, it is assumed that the integrand as a function of  $\gamma, \gamma', \gamma_1, \gamma_2, \gamma'_1$  and  $\gamma'_2$ , vanishes on the semi circle at  $\infty$ , such that it is sufficient just to replace for each integration over the conformal variables  $\gamma_l$ , in Eq. (3.2.3),

$$\oint_C d\gamma_l \rightarrow \int_{\epsilon-i\infty}^{\epsilon+i\infty} d\gamma_l \quad \{\gamma_l\} = \gamma, \gamma', \gamma_1, \gamma_2, \gamma'_1, \gamma'_2 \quad (3.2.4)$$

Following the definition of Eq. (2.2), one can replace the integration limits for the  $\gamma_l$  variables  $\epsilon - i\infty \leq \gamma_l \leq \epsilon + i\infty$ , with the corresponding limits of integration for the variables  $\nu_l$  ( $\{\nu_l\} = \nu, \nu', \nu_1, \nu_2, \nu'_1, \nu'_2$ ), namely  $-\infty \leq \nu_l \leq \infty$ . So in Eq. (3.2.3), one can change from the variable  $\gamma_l$  to the variable  $\nu_l$ , and re-express the integration over  $\gamma_l$  as

$$\oint_C d\gamma_l \rightarrow \int_{\epsilon-i\infty}^{\epsilon+i\infty} d\gamma_l = \int_{ia-\infty}^{ia+\infty} d\nu_l, \quad \{\nu_l\} = \nu, \nu', \nu_1, \nu_2, \nu'_1, \nu'_2 \quad (3.2.5)$$

where  $a = 1/2 - \epsilon$  is such that the contour of integration is below all singularities in  $\nu_l$ . Hence, in  $\nu$  notation, Eq. (3.2.3) will be rewritten as follows, where the notation  $\int_{-\infty}^{\infty} d\nu$  is understood to be a shorthand for the contour integrals written in Eq. (3.2.5).

$$\begin{aligned}
A(\mathbb{P} \rightarrow 2\mathbb{P} \rightarrow \mathbb{P}; \text{Fig. 8}) &= \int_{-\infty}^{\infty} d\nu \nu^2 \prod_{i=1}^2 \int_{-\infty}^{\infty} d\nu_i \nu_i^2 \lambda(\nu_i) \int_{-\infty}^{\infty} d\nu'_i \nu_i'^2 \lambda(\nu'_i) \int_{-\infty}^{\infty} d\nu' \nu'^2 \int d^2 q' \\
&\times \int_{Y_W + \frac{1}{2}\delta Y_W}^Y dY_1 \int_0^{Y_{b\bar{b}} - \frac{1}{2}\delta Y_{b\bar{b}}} dY_2 g_P(\vec{k}, \vec{q} = 0; -\nu) e^{\omega(\nu)(Y-Y_1)} e^{\omega(\nu_1)(Y_1-Y_W - \frac{1}{2}\delta Y_W)} e^{\omega(\nu_2)(Y_1-Y_{b\bar{b}} - \frac{1}{2}\delta Y_{b\bar{b}})} \\
&\times e^{\omega(\nu'_1)(Y_W - \frac{1}{2}\delta Y_W - Y_2)} e^{\omega(\nu'_2)(Y_{b\bar{b}} - \frac{1}{2}\delta Y_{b\bar{b}} - Y_2)} e^{\omega(\nu')(Y_2-0)} g_P(\vec{k}_0, \vec{q} = 0; \nu') \sigma(M_W, -\nu_1, \nu'_1) \sigma(M_{b\bar{b}}, -\nu_2, \nu'_2) \\
&\times \Gamma_{3\mathbb{P}}(\vec{q} = 0, -\vec{q}' | \nu, \nu_1, \nu_2) \Gamma_{3\mathbb{P}}(\vec{q} = 0, -\vec{q}' | -\nu', -\nu'_1, -\nu'_2)
\end{aligned} \tag{3.2.6}$$

$$\begin{aligned}
\text{where} \quad \sigma(M_W, -\nu_1, \nu'_1) &= g(M_W, \vec{q} = 0; -\nu_1) g(M_W, \vec{q} = 0; \nu'_1) \sigma(M_W) \\
\text{and} \quad \sigma(M_{b\bar{b}}, -\nu_2, \nu'_2) &= g(M_{b\bar{b}}, \vec{q} = 0; -\nu_2) g(M_{b\bar{b}}, \vec{q} = 0; \nu'_2) \sigma(M_{b\bar{b}})
\end{aligned} \tag{3.2.7}$$

where the expressions for the  $\sigma(M_W)$  and  $\sigma(M_{b\bar{b}})$  are given in Eq. (2.27) and Eq. (2.29), respectively. In Eq. (3.2.6), we assume that  $Y_W > Y_{b\bar{b}}$ , and that  $q = 0$ , since we are considering the inclusive process given by Fig. 8, (see the left part of this figure). From Eq. (3.2.6), we see that it is possible to integrate over  $q'$ . This integration has been performed in Ref. [8], with the result

$$\begin{aligned}
\Gamma_{3\mathbb{P}}(q = 0, q' | \nu, \nu_1, \nu_2) &\equiv \left( \frac{2\pi\bar{\alpha}_S^2}{N_c} \right) \int d^2 k g(k, q = 0, \nu) g\left(\vec{k} + \frac{1}{2}\vec{q}', \vec{q}', \nu_1\right) g\left(\vec{k} + \frac{1}{2}\vec{q}', -\vec{q}', \nu_2\right) \\
&\xrightarrow{\nu_1 \rightarrow 0, \nu_2 \rightarrow 0} \left( \frac{2\pi\bar{\alpha}_S^2}{N_c} \right) \frac{2^{1+2i\nu} C_1(\nu) \pi^4 \left(\frac{q'^2}{4}\right)^{-1/2+i\nu-i\nu_1-i\nu_2}}{(1/2+i\nu-i\nu_1-i\nu_2)^3} + \text{function without singularities in } \nu_1 \text{ and } \nu_2
\end{aligned} \tag{3.2.8}$$

In Eq. (3.2.8), we restrict ourselves to the case of small  $\nu_1$  and  $\nu_2$  ( $\nu'_1$  and  $\nu'_2$ ), since as we will show below, the main contribution to the integral over rapidity values, stems from  $Y_1 - Y_2 \rightarrow Y$ , and small values of  $\nu_1$  and  $\nu_2$  ( $\nu'_1$  and  $\nu'_2$ ), contribute to the BFKL Pomeron exchange at high energy (see Eq. (2.15), and the discussion around this equation). From Eq. (3.2.8), the result of integrating the product of the two triple pomeron vertices, which appear in the integrand on the RHS of Eq. (3.2.6), is

$$\begin{aligned}
\int d^2 q' \Gamma_{3\mathbb{P}}(\vec{q} = 0, \vec{q}' | \nu, \nu_1, \nu_2) \Gamma_{3\mathbb{P}}(\vec{q} = 0, \vec{q}' | -\nu', -\nu'_1, -\nu'_2) &= \\
\left( \frac{2\pi\bar{\alpha}_S^2}{N_c} \right)^2 \frac{2^{2i\nu-2i\nu'} C_1(\nu) C_1(-\nu') 2\pi^9 2^{(2i\nu-2i\nu_1-2i\nu_2-2i\nu'+2i\nu'_1+2i\nu'_2)}}{(1/2+i\nu-i\nu_1-i\nu_2)^3 (1/2-i\nu'+i\nu'_1+i\nu'_2)^3} &\times \delta(\nu - \nu_1 - \nu_2 - \nu' + \nu'_1 + \nu'_2)
\end{aligned} \tag{3.2.9}$$

The Dirac delta function appearing on the RHS of Eq. (3.2.9), is absorbed in Eq. (3.2.6) by integrating over  $\nu'$ . In the course of this, the expression on the RHS of Eq. (3.2.9) reduces to

$$\left(\frac{2\pi\bar{\alpha}_S^2}{N_c}\right)^2 C_1(\nu) C_1(\nu - \nu_1 - \nu_2 + \nu'_1 + \nu'_2) 2\pi^9 (1/2 + i\nu - i\nu_1 - i\nu_2)^{-3} (1/2 + i\nu - i\nu_1 - i\nu_2)^{-3}.$$

Hence, after evaluating the integration over  $\nu'$ , and making use of the expression in Eq. (2.12), in the case where  $\vec{q} = 0$  for the pomeron couplings, gives for the RHS of Eq. (3.2.6)

$$\begin{aligned} A(\mathcal{P} \rightarrow 2\mathcal{P} \rightarrow \mathcal{P}; \text{Fig. 8}) &= 2\pi^9 \left(\frac{2\pi\bar{\alpha}_S^2}{N_c}\right)^2 \Gamma_P(k, q=0) \Gamma_P(k_0, q=0) \sigma(M_W) \sigma(M_{b\bar{b}}) \\ &\times \int_{-\infty}^{\infty} d\nu \nu^2 \prod_{i=1}^2 \int_{-\infty}^{\infty} d\nu_i \nu_i^2 \lambda(\nu_i) \int_{-\infty}^{\infty} d\nu'_i \nu_i'^2 \lambda(\nu'_i) (\nu'_1 + \nu'_2 - \nu_1 - \nu_2 + \nu)^2 \\ &\times \int_{Y_W + \frac{1}{2}\delta Y_W}^Y dY_1 \int_0^{Y_{b\bar{b}} - \frac{1}{2}\delta Y_{b\bar{b}}} dY_2 g(\vec{k}, \vec{q}=0; -\nu) e^{\omega(\nu)(Y-Y_1)} e^{(\omega(\nu_1)(Y_1-Y_W - \frac{1}{2}\delta Y_W)} e^{\omega(\nu_2)(Y_1-Y_{b\bar{b}} - \frac{1}{2}\delta Y_{b\bar{b}})} \\ &\times e^{\omega(\nu'_1)(Y_W - \frac{1}{2}\delta Y_W - Y_2)} e^{\omega(\nu'_2)(Y_{b\bar{b}} - \frac{1}{2}\delta Y_{b\bar{b}} - Y_2)} e^{\omega(\nu - \nu_1 - \nu_2 + \nu'_1 + \nu'_2)(Y_2 - 0)} \\ &\times g(M_W, -\nu_1) g(M_W, \nu'_1) g(M_{b\bar{b}}, -\nu_2) g(M_{b\bar{b}}, \nu'_2) \\ &\times C_1(\nu) C_1(\nu_1 + \nu_2 - \nu'_1 - \nu'_2 - \nu) (1/2 - i\nu + i\nu_1 + i\nu_2)^{-3} (1/2 + i\nu - i\nu_1 - i\nu_2)^{-3} \\ &\times g(\vec{k}_0, \vec{q}=0; \nu'_1 + \nu'_2 - \nu_1 - \nu_2 + \nu) \end{aligned} \quad (3.2.10)$$

where from the expression of Eq. (2.12), the product  $C_1 C_1 g g$  can be recast in the form

$$\begin{aligned} &C_1(\nu) C_1(-\nu'_1 - \nu'_2 + \nu_1 + \nu_2 - \nu) g(\vec{k}, \vec{q}=0; -\nu) g(\vec{k}_0, \vec{q}=0; \nu'_1 + \nu'_2 - \nu_1 - \nu_2 + \nu) \quad (3.2.11) \\ &\longrightarrow C_1(\nu) C_1(-\nu) C_1(\nu'_1 + \nu'_2 - \nu_1 - \nu_2 + \nu) C_1(-\nu'_1 - \nu'_2 + \nu_1 + \nu_2 - \nu) \\ &(k^2 k_0^2)^{-1/2} (16k^2)^{-i\nu} (16k_0^2)^{i\nu_1 + i\nu_2 - i\nu'_1 - i\nu'_2 + i\nu} \end{aligned}$$

Hence, it is obvious that using the relation of Eq. (2.11), the expression in Eq. (3.2.11) cancels the term  $\nu^2 (\nu'_1 + \nu'_2 - \nu_1 - \nu_2 + \nu)^2$  in the numerator of the integrand of Eq. (3.2.10), to give

$$\begin{aligned} A(\mathcal{P} \rightarrow 2\mathcal{P} \rightarrow \mathcal{P}; \text{Fig. 8}) &= \pi^8 \Sigma(k, M_W, M_{b\bar{b}}, k_0) \\ &\times \int_{-\infty}^{\infty} d\nu \prod_{i=1}^2 \int_{-\infty}^{\infty} d\nu_i \nu_i^2 \lambda(\nu_i) \int_{-\infty}^{\infty} d\nu'_i \nu_i'^2 \lambda(\nu'_i) (16k^2)^{-i\nu} (16k_0^2)^{i\nu_1 + i\nu_2 - i\nu'_1 - i\nu'_2 + i\nu} \\ &\times \int_{Y_W + \frac{1}{2}\delta Y_W}^Y dY_1 \int_0^{Y_{b\bar{b}} - \frac{1}{2}\delta Y_{b\bar{b}}} dY_2 e^{\omega(\nu)(Y-Y_1)} e^{\omega(\nu_1)(Y_1-Y_W - \frac{1}{2}\delta Y_W)} e^{\omega(\nu_2)(Y_1-Y_{b\bar{b}} - \frac{1}{2}\delta Y_{b\bar{b}})} \\ &\times e^{\omega(\nu'_1)(Y_W - \frac{1}{2}\delta Y_W - Y_2)} e^{\omega(\nu'_2)(Y_{b\bar{b}} - \frac{1}{2}\delta Y_{b\bar{b}} - Y_2)} e^{\omega(\nu_1 + \nu_2 - \nu'_1 - \nu'_2 + \nu)(Y_2 - 0)} \\ &\times g(M_W, -\nu_1) g(M_W, \nu'_1) g(M_{b\bar{b}}, -\nu_2) g(M_{b\bar{b}}, \nu'_2) (1/2 - i\nu + i\nu_1 + i\nu_2)^{-3} (1/2 + i\nu - i\nu_1 - i\nu_2)^{-3} \end{aligned} \quad (3.2.12)$$

where the factor



$$\Sigma(k, M_W, M_{b\bar{b}}, k_0) = 2\pi^9 \left( \frac{2\pi\bar{\alpha}_S}{N_c} \right)^2 \Gamma_P(k, q=0) \Gamma_P(k_0, q=0) \frac{1}{\sqrt{k^2 k_0^2}} \sigma(M_{b\bar{b}}) M_{b\bar{b}}^2 \sigma(M_W) M_W^2 \quad (3.2.13)$$

Substituting for  $g$  appearing in Eq. (3.2.12) for the form given in Eq. (2.9), the expression on the RHS of Eq. (3.2.12) becomes

$$\begin{aligned} A(\mathcal{P} \rightarrow 2\mathcal{P} \rightarrow \mathcal{P}; Fig. 8) &= \pi^{16} \Sigma(k, M_W, M_{b\bar{b}}, k_0) \\ &\times \int_{-\infty}^{\infty} d\nu \prod_{i=1}^2 \int_{-\infty}^{\infty} d\nu_i \nu_i \lambda(\nu_i) \int_{-\infty}^{\infty} d\nu'_i \nu'_i \lambda(\nu'_i) (16k^2)^{-i\nu} (16k_0^2)^{i\nu_1+i\nu_2-i\nu'_1-i\nu'_2+i\nu} \\ &\times \int_{Y_W+\frac{1}{2}\delta Y_W}^Y dY_1 \int_0^{Y_{b\bar{b}}-\frac{1}{2}\delta Y_{b\bar{b}}} dY_2 e^{\omega(\nu)(Y-Y_1)} e^{\omega(\nu_1)(Y_1-Y_W-\frac{1}{2}\delta Y_W)} e^{\omega(\nu_2)(Y_1-Y_{b\bar{b}}-\frac{1}{2}\delta Y_{b\bar{b}})} \\ &\times e^{\omega(\nu'_1)(Y_W-\frac{1}{2}\delta Y_W-Y_2)} e^{\omega(\nu'_2)(Y_{b\bar{b}}-\frac{1}{2}\delta Y_{b\bar{b}}-Y_2)} e^{\omega(\nu'_1+\nu'_2-\nu_1-\nu_2+\nu)(Y_2-0)} (16M_W^2)^{i\nu'_1-i\nu_1} (16M_{b\bar{b}}^2)^{i\nu'_2-i\nu_2} \\ &\times (1/2 - i\nu + i\nu_1 + i\nu_2)^{-3} (1/2 + i\nu - i\nu_1 - i\nu_2)^{-3} \end{aligned} \quad (3.2.14)$$

Note that due to the  $\nu_i$  and  $\nu'_i$  ( $i = 1, 2$ ) in the denominator of Eq. (2.9), inserting this expression for the  $g$ 's into Eq. (3.2.12), the  $\nu_i^2$  and  $\nu_i'^2$  in the numerator of Eq. (3.2.12) reduce to just factors of  $\nu_i$  and  $\nu'_i$  in the numerator of Eq. (3.2.12). Since  $\omega(\nu_l) > 0$  contains a minimum at  $\nu_l = 0$ , the integration over  $Y_1$  and  $Y_2$  is actually convergent, either at  $Y - Y_1 \leq 1/\omega(0)$  ( $Y_2 \leq 1/\omega(0)$ ) or at  $Y_1 - Y_W - \frac{1}{2}\delta Y_W \leq 1/\omega(0)$  ( $Y_{b\bar{b}} - \frac{1}{2}\delta Y_{b\bar{b}} - Y_2 \leq 1/\omega(0)$ ). The maximal increase with energy stems from the region where  $Y_1 \rightarrow Y$  and  $Y_2 \rightarrow 0$ . Indeed, in this region the integrand in Eq. (3.2.12) is proportional to

$$e^{\omega(\nu_1)(Y-Y_W-\frac{1}{2}\delta Y_W)} e^{\omega(\nu_2)(Y-Y_{b\bar{b}}-\frac{1}{2}\delta Y_{b\bar{b}})} \times e^{\omega(\nu'_1)(Y_W-\frac{1}{2}\delta Y_W)} e^{\omega(\nu'_2)(Y_{b\bar{b}}-\frac{1}{2}\delta Y_{b\bar{b}})} \quad (3.2.15)$$

Using Eq. (3.2.15), and evaluating the integrations over all the  $\nu$ 's in the saddle point approximation, we see that

$$A(\mathcal{P} \rightarrow 2\mathcal{P} \rightarrow \mathcal{P}; Fig. 8) \propto \exp \left( \omega(0) \left( 2Y - \frac{1}{2}\delta Y_W - \frac{1}{2}\delta Y_{b\bar{b}} \right) \right) \quad (3.2.16)$$

where the typical values of  $\nu_l$  are

$$\begin{aligned} |\nu_1| &\approx \frac{\ln(M_W^2/k_0^2)}{2(Y - Y_W - \frac{1}{2}\delta Y_W)} \ll 1; & |\nu_2| &\approx \frac{\ln(M_{b\bar{b}}^2/k_0^2)}{2(Y - Y_{b\bar{b}} - \frac{1}{2}\delta Y_{b\bar{b}})} \ll 1; \\ |\nu'_1| &\approx \frac{\ln(M_W^2/k_0^2)}{2(Y_W - \frac{1}{2}\delta Y_W)} \ll 1; & |\nu'_2| &\approx \frac{\ln(M_{b\bar{b}}^2/k_0^2)}{2(Y_{b\bar{b}} - \frac{1}{2}\delta Y_{b\bar{b}})} \ll 1; \end{aligned} \quad (3.2.17)$$

This can be seen more clearly in the argument that follows, where considering the region of integration close to the point  $\nu \rightarrow 0$ , one obtains the delta function  $\delta(Y - Y_1 + Y_2)$  in the rapidity variables.

For small  $\nu_1$  and  $\nu_2$  ( $\nu'_1$  and  $\nu'_2$ ), we have three different kinematic regions of integration: (i)  $|i\nu + 1/2| \ll \nu_1 + \nu_2$  ( $|i\nu' + 1/2| \ll \nu'_1 + \nu'_2$ ); (ii)  $|i\nu + 1/2| \gg \nu_1 + \nu_2$  ( $|i\nu' + 1/2| \gg \nu'_1 + \nu'_2$ ); and (iii)  $|i\nu + 1/2| \approx \nu_1 + \nu_2$  ( $|i\nu' + 1/2| \approx \nu'_1 + \nu'_2$ ).

### 3.2.1 Region (I): $|i\nu + 1/2| \ll \nu_1 + \nu_2$ ( $|i\nu' + 1/2| \ll \nu'_1 + \nu'_2$ )

In the first kinematic region, we have  $\Gamma_{3P} \rightarrow 1/(\nu_1 + \nu_2)^3$ . Therefore, the integral is large for values of  $|\nu| \rightarrow 1/2$ . Using Eq. (3.2.9), the integrand in Eq. (3.2.6) could be simplified in this kinematic region in the following way.

$$\begin{aligned}
A_{\text{reg. (i)}}(IP \rightarrow 2P \rightarrow IP; Fig. 8) &= 2\pi^9 \left( \frac{2\pi\bar{\alpha}_S^2}{N_c} \right)^2 \Gamma_P(k, q=0) \Gamma_P(k_0, q=0) \sigma(M_W) \sigma(M_{b\bar{b}}) \quad (3.2.1.1) \\
&\times \int_{-\infty}^{\infty} \nu^2 d\nu C_1(\nu) \prod_{i=1}^2 \int_{-\infty}^{\infty} \nu_i^2 d\nu_i \int_{-\infty}^{\infty} \nu_i'^2 d\nu_i' \int_{-\infty}^{\infty} \nu'^2 d\nu' C_1(-\nu') \frac{\delta(\nu_1 + \nu_2 - \nu'_1 - \nu'_2) 2^{2i\nu_1 + 2i\nu_2 - 2i\nu'_1 - 2i\nu'_2}}{(\nu_1 + \nu_2)^3 (\nu'_1 + \nu'_2)^3} \\
&\times g\left(\vec{k}, \vec{q}=0; -\nu\right) \int_{Y_W + \frac{1}{2}\delta Y_W}^Y dY_1 \int_0^{Y_{b\bar{b}} - \frac{1}{2}\delta Y_{b\bar{b}}} dY_2 e^{\omega(\nu)(Y-Y_1)} e^{(\omega(\nu_1)(Y_1-Y_W - \frac{1}{2}\delta Y_W))} e^{\omega(\nu_2)(Y_1-Y_{b\bar{b}} - \frac{1}{2}\delta Y_{b\bar{b}})} \\
&\times e^{\omega(\nu'_1)(Y_W - \frac{1}{2}\delta Y_W - Y_2)} e^{\omega(\nu'_2)(Y_{b\bar{b}} - \frac{1}{2}\delta Y_{b\bar{b}} - Y_2)} e^{\omega(\nu')(Y_2-0)} \\
&\times g(M_W, -\nu_1) g(M_W, \nu'_1) g(M_{b\bar{b}}, -\nu_2) g(M_{b\bar{b}}, \nu'_2) g\left(\vec{k}, \vec{q}=0; \nu'\right)
\end{aligned}$$

The BFKL eigenvalues  $\omega(\nu)$  and  $\omega(\nu')$ , (see Eq. (2.6)) increase as  $\omega(\nu) \rightarrow -\bar{\alpha}_S/(1/2 \pm i\nu)$ , and therefore, the integral over  $\nu$  takes the following form

$$\int_{-\infty - i(\epsilon-1/2)}^{+\infty - i(\epsilon-1/2)} \frac{d\nu}{2\pi} \exp\left(-\frac{\bar{\alpha}_S}{1/2 \pm i\nu} (Y - Y_1)\right) \rightarrow -\bar{\alpha}_S \int_{-\infty}^{\infty} \frac{dt}{2\pi i} \frac{e^{t(Y-Y_1)}}{t^2} = \bar{\alpha}_S (Y - Y_1) \quad (3.2.1.2)$$

where  $t = \bar{\alpha}_S/(1/2 \pm i\nu)$ . The typical  $\nu$  in this integral, is about  $\bar{\alpha}_S(Y - Y_1)$ , while we expect  $\nu_1 \approx \nu_2 \approx 1/\bar{\alpha}_S Y$ . Therefore, for region (i)  $|i\nu + 1/2|$  cannot be less than  $\nu_1 + \nu_2$ , which is in clear contradiction with our initial assumption. It means, that the first kinematic region does not contribute to the integral.

### 3.2.2 Region (II): $|i\nu + 1/2| \gg \nu_1 + \nu_2$ ( $|i\nu' + 1/2| \gg \nu'_1 + \nu'_2$ )

In the second kinematic region,  $|i\nu + 1/2| \gg \nu_1 + \nu_2$  ( $|i\nu' + 1/2| \gg \nu'_1 + \nu'_2$ ) while  $\nu_1 \approx \nu_2 \approx \nu'_1 \approx \nu'_2 \approx 1/\alpha_S Y$ . In this region, Eq. (3.2.9) reads

$$\begin{aligned}
& \int d^2 q' \Gamma_{3P} (q=0, q'|\nu, \nu_1, \nu_2) \Gamma_{3P} (q=0, q'|-\nu', -\nu'_1, -\nu'_2) \\
& \longrightarrow \left( \frac{2\pi\bar{\alpha}_S^2}{N_c} \right)^2 \frac{2\pi^9 2^{2i\nu-2i\nu'} C_1(\nu) C_1(-\nu')}{(1/2+i\nu)^3 (1/2-i\nu')^3} \delta(\nu-\nu')
\end{aligned} \tag{3.2.2.1}$$

Taking into account Eq. (3.2.2.1), the integration over  $\nu'$  is eliminated by the Dirac delta function  $\delta(\nu-\nu')$ , which appears in Eq. (3.2.2.1), such that inserting this into Eq. (3.2.6) gives the following expression

$$\begin{aligned}
& A_{\text{reg.}(ii)} (IP \rightarrow 2P \rightarrow IP; Fig. 8) = \\
& \Sigma(k, M_W, M_{b\bar{b}}, k_0) \pi^8 \int_{-\infty}^{\infty} \frac{d\nu}{(1/2+i\nu)^3 (1/2-i\nu)^3} \left( \frac{k_0^2}{k^2} \right)^{i\nu} \prod_{i=1}^2 \int_{-\infty}^{\infty} \nu_i^2 \lambda(\nu_i) d\nu_i \int_{-\infty}^{\infty} \nu_i'^2 \lambda(\nu_i') d\nu_i' \\
& \times \int_{Y_W + \frac{1}{2}\delta Y_W}^Y dY_1 \int_0^{Y_{b\bar{b}} - \frac{1}{2}\delta Y_{b\bar{b}}} dY_2 e^{\omega(\nu)(Y-Y_1+Y_2)} e^{\omega(\nu_1)(Y_1-Y_W - \frac{1}{2}\delta Y_W)} e^{\omega(\nu_2)(Y_1-Y_{b\bar{b}} - \frac{1}{2}\delta Y_{b\bar{b}})} \\
& \times e^{\omega(\nu'_1)(Y_W - \frac{1}{2}\delta Y_W - Y_2)} e^{\omega(\nu'_2)(Y_{b\bar{b}} - \frac{1}{2}\delta Y_{b\bar{b}} - Y_2)} g(M_W, -\nu_1) g(M_W, \nu'_1) g(M_{b\bar{b}}, -\nu_2) g(M_{b\bar{b}}, \nu'_2)
\end{aligned} \tag{3.2.2.3}$$

If the following definitions are made, namely

$$\begin{aligned}
Y_{\nu_1} &= Y_1 - Y_W - \frac{1}{2}\delta Y_W; \quad L_{\nu_1} = \frac{M_W^2}{k_0^2}; & Y_{\nu_2} &= Y_1 - Y_{b\bar{b}} - \frac{1}{2}\delta Y_{b\bar{b}}; \quad L_{\nu_2} = \frac{M_{b\bar{b}}^2}{k_0^2}; \\
Y_{\nu'_1} &= Y_W - \frac{1}{2}\delta Y_W - Y_2; \quad L_{\nu'_1} = \frac{M_W^2}{k_0^2}; & Y_{\nu'_2} &= Y_{b\bar{b}} - \frac{1}{2}\delta Y_{b\bar{b}} - Y_2; \quad L_{\nu'_2} = \frac{M_{b\bar{b}}^2}{k_0^2};
\end{aligned}$$

Then Eq. (3.2.2.2) can be written in the following, more compact form,

$$\begin{aligned}
& A_{\text{reg.}(ii)} (IP \rightarrow 2P \rightarrow IP; Fig. 8) = \\
& (16\pi^4)^4 \Sigma(k, M_W, M_{b\bar{b}}, k_0) \int_{Y_W + \frac{1}{2}\delta Y_W}^Y dY_1 \int_0^{Y_{b\bar{b}} - \frac{1}{2}\delta Y_{b\bar{b}}} dY_2 I_\nu I_{\nu_1} I_{\nu_2} I'_{\nu_1} I'_{\nu_2}
\end{aligned} \tag{3.2.2.4}$$

$$\text{where } I_\nu(Y - Y_1 - Y_2) = \int_{-\infty-i(\epsilon-1/2)}^{\infty-i(\epsilon-1/2)} d\nu \frac{e^{\frac{-\bar{\alpha}_S}{1/2+i\nu}(Y-Y_1+Y_2)}}{(i\nu+1/2)^3 (1/2-i\nu)^3} \left( \frac{k_0^2}{k^2} \right)^{i\nu} \tag{3.2.2.5}$$

$$\text{and where } I_{\nu_i \rightarrow 0}((Y_{\nu_i}, L_{\nu_i})) = \int_{-\infty}^{\infty} d\nu_i \nu_i e^{\omega(\nu_i) Y_{\nu_i}} (L_{\nu_i})^{i \nu_i} \quad (3.2.2.6)$$

$$\text{comparison with Eq. (2.14)} \Rightarrow I_{\nu_i \rightarrow 0}((Y_{\nu_i}, L_{\nu_i})) \xrightarrow{\nu_i \rightarrow 0} \frac{d}{d \ln L_{\nu_i}} P(L_{\nu_i}; Y_{\nu_i}) \quad (3.2.2.7)$$

$$\xrightarrow{Y_{\nu_i} \rightarrow 0} \frac{d}{d \ln L_{\nu_i}} \delta(\ln L_{\nu_i}) \quad (3.2.2.8)$$

In Eq. (3.2.2.4), we evaluate first the integrals over  $Y_1$  and  $Y_2$ , which take the following form, where in region (ii),  $\nu_1, \nu_2, \nu'_1$  and  $\nu'_2$  are considered small.

$$\begin{aligned} & \int_{Y_W + \frac{1}{2}\delta Y_W}^Y dY_1 \int_0^{Y_{b\bar{b}} - \frac{1}{2}\delta Y_{b\bar{b}}} dY_2 I_\nu I_{\nu_1} I_{\nu_2} I'_{\nu_1} I'_{\nu_2} = \int_{-\infty}^{\infty} \frac{d\nu}{(i\nu + 1/2)^3 (i\nu - 1/2)^3} \left( \frac{k_0^2}{k^2} \right)^{i\nu} \\ & \times \int_{-\infty}^{\infty} \nu_1 L_{\nu_1}^{-i\nu_1} d\nu_1 \int_{-\infty}^{\infty} \frac{\nu_2 L_{\nu_2}^{-i\nu_2} d\nu_2}{(\omega(\nu_1) + \omega(\nu_2) - \omega(\nu))} \int_{-\infty}^{\infty} \nu'_1 L_{\nu'_1}^{-i\nu'_1} d\nu'_1 \int_{-\infty}^{\infty} \frac{\nu'_2 L_{\nu'_2}^{-i\nu'_2} d\nu'_2}{(\omega(\nu'_1) + \omega(\nu'_2) - \omega(\nu))} \\ & \times e^{\omega(\nu_1)(Y - Y_W - \frac{1}{2}\delta Y_W)} e^{\omega(\nu_2)(Y - Y_{b\bar{b}} - \frac{1}{2}\delta Y_{b\bar{b}})} \left( 1 - e^{(\omega(\nu) - \omega(\nu_1) - \omega(\nu_2))(Y - Y_W - \frac{1}{2}\delta Y_W)} \right) \\ & \times e^{\omega(\nu'_1)(Y_W - \frac{1}{2}\delta Y_W)} e^{\omega(\nu'_2)(Y_{b\bar{b}} - \frac{1}{2}\delta Y_{b\bar{b}})} \left( 1 - e^{(\omega(\nu) - \omega(\nu'_1) - \omega(\nu'_2))(Y_{b\bar{b}} - \frac{1}{2}\delta Y_{b\bar{b}})} \right) \end{aligned} \quad (3.2.2.9)$$

In the limit that  $i\nu \pm 1/2 \rightarrow 0$ , then  $\omega(\nu) \rightarrow -\bar{\alpha}_S/(i\nu \pm 1/2)$ , and in our kinematic region, Eq. (3.2.2.9) reduces to the following expression

$$\begin{aligned} & \int_{Y_W + \frac{1}{2}\delta Y_W}^Y dY_1 \int_0^{Y_{b\bar{b}} - \frac{1}{2}\delta Y_{b\bar{b}}} dY_2 I_\nu I_{\nu_1} I_{\nu_2} I'_{\nu_1} I'_{\nu_2} = \frac{1}{\bar{\alpha}_S^2} \int_{-\infty}^{\infty} \frac{d\nu}{(i\nu \pm 1/2)(i\nu \mp 1/2)^3} \left( \frac{k_0^2}{k^2} \right)^{i\nu} \\ & \times \int_{-\infty}^{\infty} \nu_1 L_{\nu_1}^{-i\nu_1} d\nu_1 \int_{-\infty}^{\infty} \nu_2 L_{\nu_2}^{-i\nu_2} d\nu_2 e^{\omega(\nu_1)(Y - Y_W - \frac{1}{2}\delta Y_W)} e^{\omega(\nu_2)(Y - Y_{b\bar{b}} - \frac{1}{2}\delta Y_{b\bar{b}})} \\ & \times \left( 1 - e^{(\omega(\nu) - \omega(\nu_1) - \omega(\nu_2))(Y - Y_W - \frac{1}{2}\delta Y_W)} \right) \\ & \times \int_{-\infty}^{\infty} \nu'_1 L_{\nu'_1}^{-i\nu'_1} d\nu'_1 \int_{-\infty}^{\infty} \nu'_2 L_{\nu'_2}^{-i\nu'_2} d\nu'_2 e^{\omega(\nu'_1)(Y_{b\bar{b}} - \frac{1}{2}\delta Y_{b\bar{b}})} e^{\omega(\nu'_2)(Y_{b\bar{b}} - \frac{1}{2}\delta Y_{b\bar{b}})} \\ & \times \left( 1 - e^{(\omega(\nu) - \omega(\nu'_1) - \omega(\nu'_2))(Y_{b\bar{b}} - \frac{1}{2}\delta Y_{b\bar{b}})} \right) \end{aligned} \quad (3.2.2.10)$$

In Eq. (3.2.2.10), the integration over  $\nu$  can be taken analytically, since

$$\int_{-\infty-i(\epsilon-1/2)}^{\infty-i(\epsilon-1/2)} \frac{d\nu}{2\pi i} \frac{1}{(i\nu \pm 1/2) (1/2 \mp i\nu)^3} = 1; \quad (3.2.2.11)$$

$$\int_{-\infty-i(\epsilon-1/2)}^{\infty-i(\epsilon-1/2)} \frac{d\nu}{2\pi i} \frac{e^{-\frac{\bar{\alpha}_S}{1/2 \pm i\nu} Y_\nu}}{(i\nu \pm 1/2) (1/2 \mp i\nu)^3} \left(\frac{k_0^2}{k^2}\right)^{i\nu} \xrightarrow{k_0^2=k^2} \frac{1}{\bar{\alpha}_S} \int_{-\infty}^{\infty} \frac{dt}{2\pi t} e^{-tY_\nu} \quad (3.2.2.12)$$

$$\approx \Theta((Y - Y_1 + Y_2) + \text{terms suppressed by powers of } \bar{\alpha}_S \text{ relative to the first term (see Eq. (3.2.2.11))} \quad (3.2.2.13)$$

$$\rightarrow \frac{1}{2\pi} \left\{ \sqrt{\frac{\pi}{f_{\text{sp}}''}} \exp \left( 2\sqrt{\bar{\alpha}_S Y_\nu \ln(k^2/k_0^2)} \right) \right\} \left( 1 - \frac{\bar{\alpha}_S}{t_{\text{sp}}} \right)^{-3} \quad (3.2.2.14)$$

where  $t = -\bar{\alpha}_S/(1/2 \pm i\nu)$ , and  $\Theta(x) = 1$  if  $x > 0$  while  $\Theta(x) = 0$  for  $x < 0$ . The last integral is taken using the steepest decent method, and  $t_{\text{sp}} = \sqrt{\frac{\bar{\alpha}_S \ln(k^2/k_0^2)}{Y_i}}$  is the saddle point of the integral in Eq. (3.2.2.14).  $f_{\text{sp}}'' = t_{\text{sp}} Y_i$ . However, this method works only in the region  $Y_i t_{\text{sp}} > 1$ . For  $Y_i t_{\text{sp}} < 1$ , we can use Eq. (3.2.2.13). Using Eq. (3.2.2.13) for the calculation, we find that the largest contribution stems from the first term in both parentheses in the integrand of Eq. (3.2.2.10). Hence, the first terms in both parentheses survive, leading to the following expression

$$\begin{aligned} & \int_{Y_W + \frac{1}{2}\delta Y_W}^Y dY_1 \int_0^{Y_{bb} - \frac{1}{2}\delta Y_{bb}} dY_2 I_\nu I_{\nu_1} I_{\nu_2} I'_{\nu_1} I'_{\nu_2} = \\ & \int_{-\infty}^{\infty} \nu_1 L_{\nu_1}^{-i\nu_1} d\nu_1 \int_{-\infty}^{\infty} \nu_2 L_{\nu_2}^{-i\nu_2} d\nu_2 \int_{-\infty}^{\infty} \nu'_1 L_{\nu'_1}^{-i\nu'_1} d\nu'_1 \int_{-\infty}^{\infty} \nu'_2 L_{\nu'_2}^{-i\nu'_2} d\nu'_2 \times \\ & \times \frac{1}{\bar{\alpha}_S^2} e^{\omega(\nu_1)(Y - Y_W - \frac{1}{2}\delta Y_W)} e^{\omega(\nu_2)(Y - Y_{bb} - \frac{1}{2}\delta Y_{bb})} e^{\omega(\nu'_1)(Y_W - \frac{1}{2}\delta Y_W)} e^{\omega(\nu'_2)(Y_{bb} - \frac{1}{2}\delta Y_{bb})} \end{aligned} \quad (3.2.2.15)$$

The integrals over  $\nu_i$  and  $\nu'_i$ , lead to the Pomeron amplitudes given by Eq. (2.14), and the final answer for this kinematic region is given by the following expression.

$$A(\mathbb{P} \rightarrow 2\mathbb{P} \rightarrow \mathbb{P}; \text{Fig. 8})_{\text{reg II}} = \frac{(2\pi)^{16}}{\bar{\alpha}_S^2} \Sigma(k^2, M_W, M_{bb}, k_0) \nu_1^{SP} \nu_2^{SP} \nu'_1{}^{SP} \nu'_2{}^{SP} \times \quad (3.2.2.16)$$

$$P\left(k, M_{b,\bar{b}}|Y - Y_{bb} - \frac{1}{2}\delta Y_{bb}\right) P\left(k_0, M_{b,\bar{b}}|Y_{bb} - \frac{1}{2}\delta Y_{bb}\right) P\left(k, M_W|Y - Y_W - \frac{1}{2}\delta Y_W\right) P\left(k_0, M_W|Y_W - \frac{1}{2}\delta Y_W\right)$$

where  $\nu_i^{SP}$  is the value of the saddle point in the integration over  $\nu_i$ , in the steepest decent method, and

$$\nu_1^{SP} \nu_2^{SP} \nu'_1{}^{SP} \nu'_2{}^{SP} = \frac{\pi^2 \ln(M_W^2/k^2) \ln(M_W^2/k_0^2) \ln(M_{bb}^2/k^2) \ln(M_{bb}^2/k_0^2)}{(Y - Y_{bb} - \frac{1}{2}\delta Y_{bb}) (Y - Y_W - \frac{1}{2}\delta Y_W) (Y_{bb} - \frac{1}{2}\delta Y_{bb}) (Y_W - \frac{1}{2}\delta Y_W)}$$

### 3.2.3 Region (III): $|i\nu + 1/2| \approx \nu_1 + \nu_2$ ( $|i\nu' + 1/2| \approx \nu'_1 + \nu'_2$ )

As it has been pointed out in Ref.[8], the fastest increase with energy stems from the third region of integration over  $\nu$ ,  $\nu_1$  and  $\nu_2$ , which is specified by

$$\begin{aligned} \nu_1 &\rightarrow \nu_2; \quad 1/2 + i\nu - i\nu_1 - i\nu_2 = 0; \quad \omega(2\nu_1^0 + \frac{1}{2}i) = 2\omega(\nu_1^0) \\ \nu'_1 &\rightarrow \nu'_2; \quad 1/2 + i\nu' - i\nu'_1 - i\nu'_2 = 0; \quad \omega(2\nu_1'^0 + \frac{1}{2}i) = 2\omega(\nu_1'^0) \end{aligned} \quad (3.2.3.1)$$

It turns out, that  $2\omega(\nu_1^0) > 2\omega(0)$ , and therefore the contribution from the kinematic region specified by Eq. (3.2.3.1), leads to a faster growth than in the case of the exchange of two non interacting Pomerons. It means, that this region can lead to a larger value for the cross section for the two parton shower production at the LHC energy, in comparison with the Tevatron energy, (where such a cross section has been measured in ref. [3]). We can integrate over  $Y_1$  and  $Y_2$  in Eq. (3.2.6), to give the result

$$\begin{aligned} A(\mathbb{P} \rightarrow 2\mathbb{P} \rightarrow \mathbb{P}; Fig. 8) &= \int_{-\infty}^{\infty} d\nu \nu^2 \prod_{i=1}^2 \int_{-\infty}^{\infty} d\nu_i \nu_i^2 \lambda(\nu_i) \int_{-\infty}^{\infty} d\nu'_i \nu_i'^2 \lambda(\nu'_i) \int_{-\infty}^{\infty} d\nu' \nu'^2 \\ &\times g_P(\vec{k}, \vec{q} = 0; -\nu) \int d^2 q' \Gamma_{3\mathbb{P}}(\vec{q} = 0, \vec{q}' | \nu, \nu_1, \nu_2) \Gamma_{3\mathbb{P}}(\vec{q} = 0, \vec{q}' | -\nu', -\nu'_1, -\nu'_2) g_P(\vec{k}_0, \vec{q} = 0; \nu') \\ &\times \sigma(M_w, -\nu_1, \nu'_1) \sigma(M_{b\bar{b}}, -\nu_2, \nu'_2) (\omega(\nu_1) + \omega(\nu_2) - \omega(\nu))^{-1} (\omega(\nu') - \omega(\nu'_1) - \omega(\nu'_2))^{-1} \\ &\times \left( e^{\omega(\nu_1)(Y - Y_W - \frac{1}{2}\delta Y_W)} e^{\omega(\nu_2)(Y - Y_{b\bar{b}} - \frac{1}{2}\delta Y_{b\bar{b}})} - e^{\omega(\nu)(Y - Y_W - \frac{1}{2}\delta Y_W)} e^{\omega(\nu_2)(Y_W + \frac{1}{2}\delta Y_W - Y_{b\bar{b}} - \frac{1}{2}\delta Y_{b\bar{b}})} \right) \\ &\times \left( e^{\omega(\nu'_1)(Y_W - \frac{1}{2}\delta Y_W - Y_{b\bar{b}} + \frac{1}{2}\delta Y_{b\bar{b}})} e^{\omega(\nu')(Y_{b\bar{b}} - \frac{1}{2}\delta Y_{b\bar{b}})} - e^{\omega(\nu'_1)(Y_W - \frac{1}{2}\delta Y_W)} e^{\omega(\nu'_2)(Y_{b\bar{b}} - \frac{1}{2}\delta Y_{b\bar{b}})} \right) \end{aligned} \quad (3.2.3.2)$$

Using Eq. (3.2.7) and Eq. (3.2.9), and the expression given in the appendix (see Eq. (2.12)), we obtain

$$\begin{aligned} A(\mathbb{P} \rightarrow 2\mathbb{P} \rightarrow \mathbb{P}; Fig. 8) &= \pi^8 \Sigma(k, M_W, M_{b\bar{b}}, k) \int_{-\infty}^{\infty} d\nu \int_{-\infty}^{\infty} d\nu' \prod_{i=1}^2 \int_{-\infty}^{\infty} \nu_i^2 \lambda(\nu_i) d\nu_i \int_{-\infty}^{\infty} \nu_i'^2 \lambda(\nu'_i) d\nu'_i \\ &\times (16k_0^2)^{i\nu'} (16k^2)^{-i\nu} (16M_W^2)^{i\nu'_1 - i\nu_1} (16M_{b\bar{b}}^2)^{i\nu'_2 - i\nu_2} \delta(\nu - \nu_1 - \nu_2 - \nu' + \nu'_1 + \nu'_2) \\ &\times \frac{\left( e^{\omega(\nu_1)(Y - Y_W - \frac{1}{2}\delta Y_W)} e^{\omega(\nu_2)(Y - Y_{b\bar{b}} - \frac{1}{2}\delta Y_{b\bar{b}})} - e^{\omega(\nu)(Y - Y_W - \frac{1}{2}\delta Y_W)} e^{\omega(\nu_2)(Y_W + \frac{1}{2}\delta Y_W - Y_{b\bar{b}} - \frac{1}{2}\delta Y_{b\bar{b}})} \right)}{(1/2 - i\nu + i\nu_1 + i\nu_2)^3 (\omega(\nu_1) + \omega(\nu_2) - \omega(\nu))} \\ &\times \frac{\left( e^{\omega(\nu'_1)(Y_W - \frac{1}{2}\delta Y_W - Y_{b\bar{b}} + \frac{1}{2}\delta Y_{b\bar{b}})} e^{\omega(\nu')(Y_{b\bar{b}} - \frac{1}{2}\delta Y_{b\bar{b}})} - e^{\omega(\nu'_1)(Y_W - \frac{1}{2}\delta Y_W)} e^{\omega(\nu'_2)(Y_{b\bar{b}} - \frac{1}{2}\delta Y_{b\bar{b}})} \right)}{(1/2 + i\nu' - i\nu'_1 - i\nu'_2)^3 (\omega(\nu') - \omega(\nu'_1) - \omega(\nu'_2))} \\ &\times C_1(-\nu_1) C_1(\nu'_1) C_1(-\nu_2) C_1(\nu'_2) \end{aligned} \quad (3.2.3.3)$$

In order to evaluate the integrations over  $\nu_1$ ,  $\nu_2$ ,  $\nu'_1$  and  $\nu'_2$  on the RHS of Eq. (3.2.3.3), it will be useful to make the following change of variables. Let  $\nu_{(12)} = \frac{1}{2}(\nu_1 + \nu_2)$ , and  $\nu_{[12]} = \frac{1}{2}(\nu_1 - \nu_2)$ , and

likewise for  $\nu'_{(12)} = \frac{1}{2} (\nu_1 + \nu_2)$ , and  $\nu'_{[12]} = \frac{1}{2} (\nu'_1 - \nu'_2)$ . In new variables  $\prod_{i=1}^2 \nu_i^2 \lambda(\nu_i) d\nu_i \nu_i'^2 \lambda(\nu'_i) d\nu'_i$  has the form  $16 \left( \nu_{(12)}^2 - \nu_{[12]}^2 \right) \left( \nu_{(12)}'^2 - \nu_{[12]}'^2 \right) d\nu_{(12)} d\nu_{[12]} d\nu_{(12)}' d\nu_{[12]}'$ . We expect that  $\nu_{(12)}$  and  $\nu_{(12)}'$  will be close to  $\nu_1^0$  while both  $\nu_{[12]}$  and  $\nu_{[12]}'$  will be much smaller. Indeed, assuming this we can expand  $\omega(\nu_i) = \omega(\nu_{(12)}) + \omega'(\nu_{(12)}) \nu_{[12]} - \omega''(\nu_{(12)}) \nu_{[12]}^2/2$ . Using this expansion one can see that integrals over  $\nu_{[12]}$  and  $\nu_{[12]}'$  have a Gaussian form and can be taken using the steepest decent method. The saddle point value of these variables are small and decreasing with energy, namely,

$$\nu_{[12]}^{SP} = \frac{\ln(M_W^2 M_{bb}^2/k_0^4)}{2Y - Y_W - \frac{1}{2}\delta Y_W - Y_{bb} - \frac{1}{2}\delta Y_{bb}}; \quad \nu_{[12]}'^{SP} = \frac{\ln(M_W^2 M_{bb}^2/k_0^4)}{Y_W - \frac{1}{2}\delta Y_W + Y_{bb} - \frac{1}{2}\delta Y_{bb}}; \quad (3.2.3.4)$$

Evaluating the integrals over  $\nu_{(12)}$  and  $\nu_{(12)}'$  by closing the contour on the pole, and by using the  $\delta$  function, Eq. (3.2.3.3) reduces to the following expression (considering  $\nu_{[12]}^{SP}$  as well as  $\nu_{[12]}'^{SP}$  are small:  $\nu_{[12]}^{SP} \ll \nu_{(12)}$  and  $\nu_{[12]}'^{SP} \ll \nu_{(12)}'$ ).

$$\begin{aligned} A(\mathcal{P} \rightarrow 2\mathcal{P} \rightarrow \mathcal{P}; \text{Fig. 8}) &= \pi^8 \Sigma(k, M_W, M_{bb}, k_0) \int d\nu d\nu' \nu_1 \nu_2 d\nu_{12} \nu'_1 \nu'_2 d\nu'_{12} \\ &\times \left( \frac{k^2}{M_W^2 M_{bb}^2} \right)^{-i\nu} \left( \frac{k_0^2}{M_W^2 M_{bb}^2} \right)^{i\nu'} \frac{\omega''(0) (Y - Y_W - \frac{1}{2}\delta Y_W)}{(\omega(\nu_1) + \omega(\nu_2) - \omega(\nu)) (\omega(\nu'_1) + \omega(\nu'_2) - \omega(\nu'))} \\ &\times e^{\omega(\nu_1)(Y - Y_W - \frac{1}{2}\delta Y_W)} e^{\omega(\nu_2)(Y - Y_{bb} - \frac{1}{2}\delta Y_{bb})} \left( 1 - e^{(\omega(\nu) - \omega(\nu_1) - \omega(\nu_2))(Y - Y_W - \frac{1}{2}\delta Y_W)} \right) \\ &\times e^{\omega(\nu'_1)(Y_W - \frac{1}{2}\delta Y_W)} e^{\omega(\nu'_2)(Y_{bb} - \frac{1}{2}\delta Y_{bb})} \left( 1 - e^{(\omega(\nu') - \omega(\nu'_1) - \omega(\nu'_2))(Y_{bb} - \frac{1}{2}\delta Y_{bb})} \right) \end{aligned} \quad (3.2.3.5)$$

In this integral  $\nu_{(12)} = \frac{1}{2}(\nu - \frac{1}{2}i)$  and  $\nu_{(12)}' = \frac{1}{2}(\nu' - \frac{1}{2}i)$  and  $\nu_i = \frac{1}{2}(\nu - \frac{1}{2}i) \pm \nu_{[12]} \rightarrow \nu_1^0$  at high energy, as well as  $\nu'_i = \frac{1}{2}(\nu' - \frac{1}{2}i) \pm \nu'_{[12]} \rightarrow \nu_1^0$ . It should be stressed, that in Eq. (3.2.3.5), all the  $\nu$ 's satisfy Eq. (3.2.3.1). Expanding  $\omega(\nu_i)$  around the point in the vicinity of  $\nu_1 = \nu'_1 = \nu_1^0$ , and denoting  $i\nu_1 - i\nu_1^0 = f$  and  $i\nu_1 - i\nu_1^0 = f'$ , we find that Eq. (3.2.10) can be written as follows

$$\begin{aligned} &\int_{\epsilon - i\infty}^{\epsilon + i\infty} \frac{df}{2\pi i} e^{(\omega(\nu_1^0) + \tilde{d}f/2)(2Y - Y_W - Y_{bb} - \frac{1}{2}(\delta Y_W + \delta Y_{bb}))} \frac{1}{df} \left( 1 - e^{-df(Y - Y_W - \frac{1}{2}\delta Y_W)} \right) \\ &\int_{\epsilon - i\infty}^{\epsilon + i\infty} \frac{df'}{2\pi i} e^{(\omega(\nu_1^0) + \tilde{d}f'/2)(Y_W + Y_{bb} - \frac{1}{2}(\delta Y_W + \delta Y_{bb}))} \frac{1}{df'} \left( 1 - e^{-df'(Y_{bb} + \frac{1}{2}\delta Y_{bb})} \right) \end{aligned} \quad (3.2.3.6)$$

where  $\tilde{d} \equiv 2\omega''(\nu_1 = \nu_1^0) > 0$  and  $d \equiv \tilde{d} - \omega''(2\nu_1^0 + i1/2) > \tilde{d}$ . In this integral, we can close the contour of integration over  $f$  and  $f'$ , on the poles  $f = 0$  and  $f' = 0$ , for the first term in each set of parentheses. In all other terms in Eq. (3.2.3.6), we can close the contour on the right semi-plane, where we have no singularities, and therefore these integrals are equal to zero. Finally, we have

$$A(\mathcal{P} \rightarrow 2\mathcal{P} \rightarrow \mathcal{P}; Fig. 8) = \pi^8 \Sigma(k, M_W, M_{b\bar{b}}, k_0) \quad (3.2.3.7)$$

$$\begin{aligned} & \frac{(\nu_1^0)^4}{d^2} \int \frac{d\nu_{12} d\nu'_{12}}{\sqrt{k_0^2 M_W^2 M_{b\bar{b}}^2}} \left( \frac{k^2}{\sqrt{M_W^2 M_{b\bar{b}}^2}} \right)^{2\nu_1^0} \left( \frac{k_0^2}{\sqrt{M_W^2 M_{b\bar{b}}^2}} \right)^{2\nu_1^0} \omega''(0) (Y - Y_W - \frac{1}{2}\delta Y_W) \\ & \times e^{\omega(\nu_1^0 + \frac{1}{2}\nu_{12})(Y - Y_W - \frac{1}{2}\delta Y_W)} e^{\omega(\nu_1^0 - \frac{1}{2}\nu_{12})(Y - Y_{b\bar{b}} - \frac{1}{2}\delta Y_{b\bar{b}})} e^{\omega(\nu_1^0 + \frac{1}{2}\nu'_{12})(Y_W - \frac{1}{2}\delta Y_W)} e^{\omega(\nu_1^0 - \frac{1}{2}\nu'_{12})(Y_{b\bar{b}} - \frac{1}{2}\delta Y_{b\bar{b}})} \end{aligned}$$

( in Eq. (3.2.3.7), we hope that the factor  $d$  will be not confused with the sign of the differential)  
Expanding  $\omega(\nu_1^0 + \frac{1}{2}\nu_{12})$  and  $\omega(\nu_1^0 + \frac{1}{2}\nu'_{12})$  for the case of small  $\nu_{12}$  ( $\nu'_{12}$ ), and integrating over  $\nu_{12}$  and  $\nu'_{12}$ , we obtain

$$\begin{aligned} A(\mathcal{P} \rightarrow 2\mathcal{P} \rightarrow \mathcal{P}; Fig. 8) &= \pi^9 \Sigma(k, M_W, M_{b\bar{b}}, k_0) \frac{(\nu_1^0)^4}{d^2} \left( \frac{k^2}{\sqrt{M_W^2 M_{b\bar{b}}^2}} \right)^{2\nu_1^0} \left( \frac{k_0^2}{\sqrt{M_W^2 M_{b\bar{b}}^2}} \right)^{2\nu_1^0} \\ & \times \omega''(0) (Y - Y_W - \frac{1}{2}\delta Y_W) \exp\left(2\omega(\nu_1^0)(Y - \frac{1}{2}(\delta Y_W + \delta Y_{b\bar{b}}))\right) \\ & \times \frac{1}{\sqrt{2\omega''(0)(2Y - Y_W - Y_{b\bar{b}})}} \exp\left(-\frac{\ln^2(M_W M_{b\bar{b}}/k^2)}{2\omega''(0)(2Y - (Y_W + Y_{b\bar{b}}))}\right) \\ & \times \frac{1}{\sqrt{2\omega''(0)(Y_W + Y_{b\bar{b}})}} \exp\left(-\frac{\ln^2(M_W M_{b\bar{b}}/k_0^2)}{2\omega''(0)(Y_W + Y_{b\bar{b}})}\right) \end{aligned} \quad (3.2.3.8)$$

Eq. (3.2.3.8) can be rewritten in a simpler way, namely

$$\begin{aligned} A(\mathcal{P} \rightarrow 2\mathcal{P} \rightarrow \mathcal{P}; Fig. 8)_{\text{reg. III}} &= \pi^9 \Sigma(k, M_W, M_{b\bar{b}}, k_0) \frac{(\nu_1^0)^4}{d^2} \left( \frac{k^2}{\sqrt{M_W^2 M_{b\bar{b}}^2}} \right)^{2\nu_1^0} \left( \frac{k_0^2}{\sqrt{M_W^2 M_{b\bar{b}}^2}} \right)^{2\nu_1^0} \\ & \times \omega''(0) (Y - Y_W - \frac{1}{2}\delta Y_W) \exp\left(2(\omega(\nu_1^0) - \omega(0))\left(Y - \frac{1}{2}(\delta Y_W + \delta Y_{b\bar{b}})\right)\right) \\ & \times P\left(k, \sqrt{M_W M_{b\bar{b}}}|2Y - Y_W - Y_{b\bar{b}} - \frac{1}{2}(\delta Y_W - \delta Y_{b\bar{b}})\right) P\left(k_0, \sqrt{M_W M_{b\bar{b}}}|Y_W + Y_{b\bar{b}} - \frac{1}{2}(\delta Y_W - \delta Y_{b\bar{b}})\right) \end{aligned} \quad (3.2.3.9)$$

### 3.2.4 Region (IV): $\nu \ll 1$ , $\nu_1 \ll 1$ and $\nu_2 \ll 1$ ( $\nu' \ll 1$ , $\nu'_1 \ll 1$ and $\nu'_2 \ll 1$ )

In our previous calculations, we focused our efforts on the singular part of  $\Gamma_{3\mathcal{P}}(q=0, q'|\nu, \nu_1, \nu_2) \equiv \left(\frac{2\pi\bar{\alpha}_S^2}{N_c}\right) \int d^2k g(k, q=0, \nu) g\left(\vec{k} + \frac{1}{2}\vec{q}', \vec{q}', \nu_1\right) g\left(\vec{k} + \frac{1}{2}\vec{q}', -\vec{q}', \nu_2\right)$  (see Eq. (3.2.8)). However, the integral in the region where all the  $\nu$ 's are small, also can lead to a contribution which increases at large values of  $Y$ , as  $\exp(\omega(0)(2Y - \frac{1}{2}\delta Y_W - \frac{1}{2}\delta Y_{b\bar{b}}))$ . Indeed, in this kinematic region we can integrate Eq. (3.2.1.2)



over all  $\nu_i$  ( $\nu'_i$ ), using the expansion of Eq. (2.15). As an example, the  $\nu_1$  integration in Eq. (3.2.14) takes the following form, using the expansion of Eq. (2.15).

$$\int_{-\infty}^{\infty} d\nu_1 \nu_1 \lambda(\nu_1) e^{\omega(0)(Y_1 - Y_W - \frac{1}{2}\delta Y_W) + \frac{1}{2}\nu_1^2 \omega''(0)(Y_1 - Y_W - \frac{1}{2}\delta Y_W) - i\nu_1 \ln(M_W^2/k^2)} \quad (3.2.4.1)$$

The exponential has a saddle point at the point  $\nu_1^{\text{sp}} = i \ln(M_W^2/k_0^2) / (\omega''(0)(Y_1 - Y_W - \frac{1}{2}\delta Y_W))$ . The expression in the exponential  $f(\nu_1)$ , at the saddle point takes the value  $f(\nu_1^{\text{sp}}) = \frac{1}{2} \ln^2(M_W^2/k^2) / (\omega''(0)(Y_1 - Y_W - \frac{1}{2}\delta Y_W))$ . Hence, evaluating the integration in Eq. (3.2.4.1), using the method of steepest descents gives the following result.

$$16 \nu_1^{\text{sp}} e^{\omega(0)(Y_1 - Y_W - \frac{1}{2}\delta Y_W)} \times e^{f(\nu_1^{\text{sp}})} \left( \frac{2\pi}{f''(\nu_1^{\text{sp}})} \right)^{1/2} = 16 \frac{i \ln(M_W^2/k_0^2)}{(\omega''(0)(Y_1 - Y_W - \frac{1}{2}\delta Y_W))} \quad (3.2.4.2)$$

$$\times e^{\omega(0)(Y_1 - Y_W - \frac{1}{2}\delta Y_W)} \times e^{\frac{1}{2} \ln^2(M_W^2/k_0^2) (\omega''(0)(Y_1 - Y_W - \frac{1}{2}\delta Y_W))^{-1}} \times \left( \frac{2\pi}{\omega''(0)(Y_1 - Y_W - \frac{1}{2}\delta Y_W)} \right)^{1/2}$$

where  $f''(\nu_1^{\text{sp}}) = \omega''(0)(Y_1 - Y_W - \frac{1}{2}\delta Y_W)$ . The factor of 16 in front in Eq. (3.2.4.2), originates from the value which  $\lambda(\nu_1)$  appearing in Eq. (3.2.4.1) takes at small  $\nu_1$ , (see Eq. (2.8)). The integration over the  $\nu_1$ ,  $\nu'_1$  and  $\nu'_2$ , are evaluated in a similar way, using the method of steepest descents. Hence, the result after integration of the RHS of Eq. (3.2.1.2), can be written as follows

$$A(\mathcal{P} \rightarrow 2\mathcal{P} \rightarrow \mathcal{P}; \text{Fig. 8})_{\text{reg (iv)}} = (16\pi^4)^4 \Sigma(k, M_W, M_{b\bar{b}}, k_0) \quad (3.2.4.3)$$

$$\times \int_{Y_W + \frac{1}{2}\delta Y_W}^Y dY_1 \int_0^{Y_{b\bar{b}} - \frac{1}{2}\delta Y_{b\bar{b}}} dY_2 e^{\omega(0)(Y - Y_1 + Y_2)} e^{2\omega(0)(Y_1 - Y_2 - \frac{1}{2}\delta Y_W - \frac{1}{2}\delta Y_{b\bar{b}})}$$

$$\times \left( \frac{2\pi}{\omega''(0)(Y - Y_1)} \right)^{1/2} \left( \frac{2\pi}{\omega''(0)(Y_2 - 0)} \right)^{1/2} \ln^2(M_W^2/k_0^2) \ln^2(M_{b\bar{b}}^2/k_0^2)$$

$$\times 2\pi \left\{ \omega''(0) \left( Y_1 - Y_W - \frac{1}{2}\delta Y_W \right) \omega''(0) \left( Y_W - \frac{1}{2}\delta Y_W - Y_2 \right) \right\}^{-3/2}$$

$$\times 2\pi \left\{ \omega''(0) \left( Y_1 - Y_{b\bar{b}} - \frac{1}{2}\delta Y_{b\bar{b}} \right) \omega''(0) \left( Y_{b\bar{b}} - \frac{1}{2}\delta Y_{b\bar{b}} - Y_2 \right) \right\}^{-3/2}$$

$$\times \exp \left( -\frac{1}{2} \frac{\ln^2(M_W^2/k_0^2)}{\omega''(0)(Y_1 - Y_W - \frac{1}{2}\delta Y_W)} \right) \exp \left( -\frac{1}{2} \frac{\ln^2(M_W^2/k_0^2)}{\omega''(0)(Y_W - \frac{1}{2}\delta Y_W - Y_2)} \right)$$

$$\times \exp \left( -\frac{1}{2} \frac{\ln^2(M_{b\bar{b}}^2/k_0^2)}{\omega''(0)(Y_1 - Y_{b\bar{b}} - \frac{1}{2}\delta Y_{b\bar{b}})} \right) \exp \left( -\frac{1}{2} \frac{\ln^2(M_{b\bar{b}}^2/k_0^2)}{\omega''(0)(Y_{b\bar{b}} - \frac{1}{2}\delta Y_{b\bar{b}} - Y_2)} \right)$$

The largest contribution to the integrals over  $Y_1$  and  $Y_2$ , stems from the region  $Y - Y_1 \propto 1/\omega(0)$ , and  $Y_2 - 0 \propto 1/\omega(0)$ . Since  $\omega''(0)/\omega(0) \approx 1$ , as far as the QCD coupling is concerned, we can conclude from Eq. (3.2.4.3) that (using the Eq. (2.17) for the expression for  $P(k, k_0|Y - Y')$ , for the case of small  $\nu$ )

$$\begin{aligned}
A(\mathcal{P} \rightarrow 2\mathcal{P} \rightarrow \mathcal{P}; Eq. (3.2.4.3))_{\text{reg. IV}} &\propto (2\pi)^{16} \Sigma(k, M_W, M_{b\bar{b}}, k_0) \\
&\times \frac{\pi^2 \ln(M_W^2/k_0^2) \ln(M_W^2/k_0^2) \ln(M_{b\bar{b}}^2/k_0^2) \ln(M_{b\bar{b}}^2/k_0^2)}{(Y - Y_{b\bar{b}} - \frac{1}{2}\delta Y_{b\bar{b}}) (Y - Y_W - \frac{1}{2}\delta Y_W) (Y_{b\bar{b}} - \frac{1}{2}\delta Y_{b\bar{b}}) (Y_W - \frac{1}{2}\delta Y_W)} P\left(k, M_{b,\bar{b}}|Y - Y_{b\bar{b}} - \frac{1}{2}\delta Y_{b\bar{b}}\right) \\
&\times P\left(k_0, M_{b,\bar{b}}|Y_{b\bar{b}} - \frac{1}{2}\delta Y_{b\bar{b}}\right) P\left(k, M_W|Y - Y_W - \frac{1}{2}\delta Y_W\right) P\left(k_0, M_W|Y_W - \frac{1}{2}\delta Y_W\right)
\end{aligned} \tag{3.2.4.4}$$

Comparing this contribution with Eq. (3.2.2.16), one can see that

$$\frac{A(\mathcal{P} \rightarrow 2\mathcal{P} \rightarrow \mathcal{P}; Eq. (3.2.4.4))_{\text{reg IV}}}{A(\mathcal{P} \rightarrow 2\mathcal{P} \rightarrow \mathcal{P}; Eq. (3.2.2.16))_{\text{reg II}}} \propto \bar{\alpha}_S^2 \ll 1 \tag{3.2.4.5}$$

Therefore, this kinematic region gives a much smaller contribution, than the kinematic region (II).

#### 4. Estimates of the background

Comparing Eq. (3.2.2.16) with Eq. (3.2.3.9), one can see that the first contribution is suppressed. Indeed, the ratio of these two contributions for  $Y_W = Y_{b\bar{b}} = 0$  in the c.m.f., is equal to

$$\begin{aligned}
\frac{A(\mathcal{P} \rightarrow 2\mathcal{P} \rightarrow \mathcal{P}; Eq. (3.2.3.9))_{\text{reg III}}}{A(\mathcal{P} \rightarrow 2\mathcal{P} \rightarrow \mathcal{P}; Eq. (3.2.2.16))_{\text{reg II}}} &= \bar{\alpha}_S^2 \omega''^2(0) (Y/2 - \frac{1}{2}\delta Y_W) (Y/2 - \frac{1}{2}\delta Y_{b\bar{b}}) \frac{(\nu_1^0)^4}{d^2 \nu_1^{SP} \nu_2^{SP} \nu_1'^{SP} \nu_2'^{SP}} \\
&\times \exp\left(2 (\omega(\nu_1^0) - \omega(0)) \left(Y - \frac{1}{2}(\delta Y_W + \delta Y_{b\bar{b}})\right)\right) \gg 1 \tag{4.1}
\end{aligned}$$

Indeed, the main factor that determines the energy behavior, is  $\exp(2 (\omega(\nu_1^0) - \omega(0)) (Y - \frac{1}{2}(\delta Y_W + \delta Y_{b\bar{b}}))) \gg 1$  which increases with energies. Other factors include  $\omega''^2(0)/d^2 \approx 1/4$ , and  $\bar{\alpha}_S (Y/2 - \frac{1}{2}\delta Y_W) \gg 1$ , as well as  $\bar{\alpha}_S (Y/2 - \frac{1}{2}\delta Y_{b\bar{b}}) \gg 1$ . However, at high energy  $\nu_1^0/\nu_1^{SP} \gg 1$ . This factor cannot change the asymptotic behavior of this ratio, but it leads to a decrease in the range of energy that we are interested in, namely from the Tevatron to the LHC energy.

It turns out, that both at the Tevatron and the LHC energies, the ratio of Eq. (4.1) is smaller than unity, since  $\nu_1^{SP}$  is equal to 0.37 and 0.19, respectively, if we take  $\alpha_S = \alpha_S(M_H k_0)$ , and  $k_0 = 1 \text{ GeV}$ . Such values of  $\nu_{SP}$  lead to  $\nu_1^0/\nu_1^{SP} = 0.21$  at the Tevatron, and  $\nu_1^0/\nu_1^{SP} = 0.42$  at the LHC. The numerical solution of Eq. (3.2.3.1), gives the following relation (see Ref. [8])

$$2(\omega(\nu_1^0) - \omega(0)) \approx 0.25 \bar{\alpha}_S \tag{4.2}$$

which leads to  $\exp(2(\omega(\nu_1^0) - \omega(0))(Y - \frac{1}{2}(\delta Y_W + \delta Y_{b\bar{b}}))) \approx 1.4$  (for the Tevatron) and 1.86 for the LHC. Collecting these, estimate we obtain that the ratio of Eq. (4.1) to be equal to  $7 \times 10^{-4}$  for the Tevatron, and  $1.4 \times 10^{-2}$  for the LHC. It means that we can neglect the contribution of Eq. (3.2.3.9), and consider only the contribution given by Eq. (3.2.2.16), which describes the production of the  $W$  boson, and the  $b\bar{b}$ -pair from two parton showers.

In this paper, we obtain two different expression for the two parton shower production, namely Eq. (3.1.3) for the non-enhanced diagram, and Eq. (3.2.2.16) for the enhanced diagram. From a purely theoretical point of view, it has been proven [13, 14], that the only contribution stems from the enhanced diagram, which reproduces the non-enhanced diagram in the low energy limit ( $Y - y_1 \approx 1/\alpha_S, y_2 \approx 1/\alpha_S$ ), at least for the case of dipole-dipole scattering. In this case, their contribution given by Eq. (3.2.2.16), has been measured at the Tevatron [3], and it's value at the LHC energy can be estimated using the following expression

$$\begin{aligned} \frac{d^2\sigma(p+p \rightarrow W + [b\bar{b}] + X)}{dY_W dY_{b\bar{b}}} &= \frac{1}{2\sigma_{eff}} \frac{\nu_1^{SP}(\text{LHC}) \nu_2^{SP}(\text{LHC}) \nu_1'^{SP}(\text{LHC}) \nu_2'^{SP}(\text{LHC})}{\nu_1^{SP}(\text{Tevatron}) \nu_2^{SP}(\text{Tevatron}) \nu_1'^{SP}(\text{Tevatron}) \nu_2'^{SP}(\text{Tevatron})} \\ &\times \frac{d\sigma_{incl}(\ln(s/M_{b,\bar{b}}^2); Y_{b\bar{b}}; 0)}{dY_{b\bar{b}}} \frac{d\sigma_{incl}(\ln(s/M_W^2); Y_W; 0)}{dY_W} \\ &\approx \frac{1}{16\sigma_{eff}} \frac{d\sigma_{incl}(\ln(s/M_{b,\bar{b}}^2); Y_{b\bar{b}}; 0)}{dY_{b\bar{b}}} \frac{d\sigma_{incl}(\ln(s/M_W^2); Y_W; 0)}{dY_W} \end{aligned} \quad (4.3)$$

The ratio of this background to the signal, can be written as follows

$$\frac{M_{b\bar{b}}^2 \frac{d^2\sigma(p+p \rightarrow W + [b\bar{b}] + X)}{dY_W dY_{b\bar{b}}}}{\frac{d^2\sigma(p+p \rightarrow W + H + X)}{dY_W dY_H}} = \frac{\frac{d\sigma_{incl}(p+p \rightarrow W + X)}{dY_W}}{\frac{d^2\sigma_{incl}(p+p \rightarrow W + H + X)}{dY_W dY_H}} \frac{1}{16\sigma_{eff}} M_{b\bar{b}}^2 \frac{d^2\sigma_{incl}(p+p \rightarrow b\bar{b} + X)}{dM_{b\bar{b}}^2 dY_{b\bar{b}}} \quad (4.4)$$

The first factor in Eq. (4.4) is well known (see Eq. (1.1)), and the uncertainties in the values of the gluon structure function does not affect it, to within an accuracy of 7%. To evaluate the cross section  $M_{b\bar{b}}^2 \frac{d^2\sigma_{incl}(p+p \rightarrow b\bar{b} + X)}{dM_{b\bar{b}}^2 dY_{b\bar{b}}}$ , we rewrite this expression as follows

$$M_{b\bar{b}}^2 \frac{d^2\sigma_{incl}(p+p \rightarrow b\bar{b} + X)}{dM_{b\bar{b}}^2 dY_{b\bar{b}}} = \frac{\sigma(M_{b\bar{b}}^2)}{\sigma(M_H^2)} \frac{d\sigma(p+p \rightarrow H + X)}{dY_H} \quad (4.5)$$

The values of  $\sigma(M_{b\bar{b}}^2)$  and  $\sigma(M_H^2)$  are calculated in Appendix 2 and Appendix 3 and it is equal to

$$\frac{\sigma(M_{b\bar{b}}^2)}{\sigma(M_H^2)} = \frac{4}{3} \frac{32\alpha_S^2}{M_{b\bar{b}}^2 A^2} \ln(M_{b\bar{b}}^2/4m_b^2) \approx 357 \quad (4.6)$$

We believe that this ratio, which we obtain in LO QCD, does not depend on the accuracy of our calculation, and will be almost the same as in the NLO approximation of perturbative QCD. All the uncertainties related to the calculations in high order perturbative QCD in Eq. (4.5), are absorbed in the value of the inclusive Higgs cross section. For this value, we take  $3 \times 10^{-9}$  mb (for LO QCD), and  $5 \times 10^{-9}$  mb (for NLO QCD) (see Refs. [16]). Substituting this value and Eq. (4.6) into Eq. (4.5), we obtain

$$M_{bb}^2 \frac{d^2 \sigma_{incl}(p+p \rightarrow b\bar{b} + X)}{dM_{bb}^2 dY_{b\bar{b}}} = (1 \div 2) \times 10^{-6} \text{ mb} \quad (4.7)$$

Using this value, we estimate the background-to-signal ratio, as

$$\frac{M_{bb}^2 \frac{d^3 \sigma(p+p \rightarrow W+[b\bar{b}]+X)}{dY_W dY_{b\bar{b}}}}{\frac{d\sigma(p+p \rightarrow W+H+X)}{dY_W dY_H}} = \frac{1.24 \div 2.4}{16} \quad (4.8)$$

Therefore, if Eq. (3.2.2.16) is responsible for the two parton shower production, the background in the LHC kinematic region will be small, and it can be neglected.

However, if the proton has some non-perturbative contribution, and differs from the colourless dipole of perturbative QCD, we can hope that the non-enhanced diagram gives the main contribution, leading to

$$\frac{M_{bb}^2 \frac{d^3 \sigma(p+p \rightarrow W+[b\bar{b}]+X)}{dY_W dY_{b\bar{b}}}}{\frac{d\sigma(p+p \rightarrow W+H+X)}{dY_W dY_H}} = 1.24 \div 2.4 \quad (4.9)$$

The background of Eq. (4.9), should be considered. However, using the fact that the production from the two parton showers does not depend on rapidity, while the signal leads to the sharp rapidity distribution in the rapidity of the  $b\bar{b}$  pair, the background can be easily separated. We would like to draw your attention to the fact that all our estimates, are heavily based on the beautiful measurement, of the so called double parton cross section, by the CDF collaboration. We would like to draw the attention of experimentalists, to the fact that this kind of measurements in the LHC region, will clarify the value of the contribution of the two parton shower processes, and therefore, will lead to an improvement of our knowledge of the non-traditional QCD background.

## 5. Summary

This paper has two main results. The first, are the estimates of the background to the associate W Higgs production. The second result, is the detailed calculation of the contribution of the enhanced diagrams to this background. As far as practical estimates are concerned, Eq. (4.8) and Eq. (4.9) give the main conclusions of this paper. These results are encouraging, since the background turns out to be no larger, than a factor 2 larger than the signal. The principle difference between the signal and background, is the dependence with respect to the rapidity difference  $Y_W - Y_{b\bar{b}}$ . The signal has a peak at  $Y_W - Y_{b\bar{b}} = 0$ ,

while the background does not depend on this difference. Having this in mind, we can easily separate this background for the signal.

The theoretical calculations, are the first where all kinematic regions in the enhanced diagram have been considered. The most interesting part, is related to the calculation of the contribution of the overlapping singularities. Being interesting theoretically, these singularities give a negligible contribution at the LHC energies and below. We believe, that this is an important observation for practical estimates of the processes, that are responsible for physics in the saturation domain.

We would like to draw the attention of experimentalists, to the fact that the measurement of the so called double parton cross section in the LHC range of energies, in the way that the CDF collaboration did at the Tevatron, will clarify both the contribution to the background of such non-traditional QCD processes as the two parton shower production, and the importance of the shadowing corrections for semihard processes.

We hope that our paper will be useful for planning experiments, in the search for the Higgs boson.

## Acknowledgments

We want to thank Asher Gotsman, Uri Maor and Alex Prygarin for very useful discussions on the subject of this paper.

This research was supported in part by the Israel Science Foundation, founded by the Israeli Academy of Science and Humanities, by a grant from the Ministry of Science, Culture & Sport, Israel & the Russian Foundation for Basic research of the Russian Federation, and by BSF grant # 20004019. One of us (E.L.), wants to thank Humboldt Foundation for financial support, that allowed him to start this paper during his visit to DESY.

## A. Appendix

### A.1 The amplitude for the subprocess in $GG \rightarrow W$

The aim of this section of the appendix, is to derive the expression for the cross section  $\sigma(M_{b\bar{b}})$ , for the production of the  $b\bar{b}$  quark - anti quark pair, in the gluon fusion  $GG \rightarrow b\bar{b}$ . These cross sections, have been calculated (see Refs.[17, 18, 19]), but we reproduce the calculation here in our technique using Sudakov variables, since using this method of calculation, it is easier to include the calculated cross sections in the framework of our approach, based on the BFKL Pomeron.

In Fig. 5, one can see that in the Born diagram for this process, the hexagon is on shell, as well as the protons between the t-channel gluons. In other words, the dashed line through the center of the diagram, intersects lines representing particles which are on shell. The cross section which corresponds to this diagram, is equal to

$$\frac{d\sigma^{BA}}{dY_W} = \frac{1}{4s} A(\text{Mueller diagram of Fig. 5 for process } p p W \rightarrow p p W) \delta\left(\frac{1}{2}\ln(\alpha_1/\beta_2) - y_W\right) \quad (\text{A.1.1})$$

where  $\alpha$  and  $\beta$  are the Sudakov variables for the vectors  $\vec{q}_1$  and  $\vec{q}_2$  ( see below). The upper line of the diagram gives the factor

$$\left(\frac{-ig_s}{q_1^2}\right) \bar{u}(p_1, s_1) \gamma^\mu u(p_1 - q_1, s'_1) \times \left(\frac{-ig_s}{q_1^2}\right) \bar{u}(p_1 - q_1, s'_1) \gamma^\rho u(p_1, s_1'') \quad (\text{A.1.2})$$

where  $s_1$ ,  $s'_1$  and  $s_1''$  are the helicities of the incoming, the intermediate, and the outgoing quarks respectively. Throughout this calculation, the Eikonal approximation is used, which assumes that the components of the momentum of the exchanged gauge particle, (in this case gluons), are small compared with the momentum of the emitting quark. Hence, in the Eikonal approach, all components of  $\vec{q}_1$  are assumed to be small, such that Eq. (A.1.2) may be replaced by

$$\left(\frac{4\pi\alpha_S}{q_1^4}\right) \bar{u}(p_1, s_1) \gamma^\mu u(p_1, s'_1) \times \bar{u}(p_1, s'_1) \gamma^\rho u(p_1, s_1'') \quad (\text{A.1.3})$$

For spinors which are normalised such that  $u(p_1, s'_1) u^\dagger(p_1, s_1) = \delta_{s_1, s'_1}$ , and using the following property of Dirac spinors from Gordon's relation, namely

$$2\bar{u}(p, s) \gamma^\mu u(p', s') = \bar{u}(p, s) \left( (p + p')^\mu + i\sigma^{\mu\nu} (p - p')_\nu \right) u(p', s') \quad (\text{A.1.4})$$

then plugging this into Eq. (A.1.3), one has for the contribution of the upper line of the diagram

$$\frac{(4\pi\alpha_S)}{q_1^4} p_1^\mu p_1^\rho \delta_{s_1, s'_1} \delta_{s'_1, s_1''} = \frac{(4\pi\alpha_S)}{q_1^4} \frac{q_{1,\perp}^\mu}{\alpha_1} \frac{q_{1,\perp}^\rho}{\alpha_1} \delta_{s_1, s'_1} \delta_{s'_1, s_1''} \quad (\text{A.1.5})$$

where we use the gauge invariant condition, that  $q_1^\mu H_{\mu,\rho,\nu,\sigma} = 0$ , where  $H$  is the amplitude of the hexagon. Similarly, the lower line of the diagram in the Eikonal approximation, gives the following contribution to the amplitude

$$\frac{(4\pi\alpha_S)}{q_2^4} p_2^\nu p_2^\sigma \delta_{s_2, s'_2} \delta_{s'_2, s_2''} = \frac{(4\pi\alpha_S)}{q_2^4} \frac{q_{2,\perp}^\nu}{\beta_2} \frac{q_{2,\perp}^\sigma}{\beta_2} \delta_{s_2, s'_2} \delta_{s'_2, s_2''} \quad (\text{A.1.6})$$

Hence, the expression for the amplitude of the diagram shown in Fig. 5, is given by the following expression, where it is assumed that the on shell quarks (horizontal lines in the hexagon shown in Fig. 5), carry momenta which depend mostly on the longitudinal direction, and all other quark lines in the hexagon, carry momenta which depend mostly on the transverse direction,

$$\begin{aligned}
A(\text{Fig. 5}) &= \frac{(4\pi\alpha_S(q^2))^2}{q_1^4 q_2^4 \alpha_1^2 \beta_2^2} \int \frac{d^4 k}{(2\pi)^4} \int \frac{d^4 l}{(2\pi)^4} H \\
&\times (2\pi)^2 \delta\left(-\beta_k \alpha_1 s - \left(\vec{k} - \vec{q}_1\right)_\perp^2 - m_u^2\right) \delta\left(\alpha_l \beta_2 s - \left(\vec{l} + \vec{q}_2\right)_\perp^2 - m_d^2\right)
\end{aligned} \tag{A.1.7}$$

$$\begin{aligned}
\text{where } H &\equiv q_{1,\perp}^\mu, q_{1,\perp}^\rho, q_{2,\perp}^\nu, q_{2,\perp}^\sigma H_{\mu\rho\nu\sigma} \\
&= \frac{f(M_W)}{D_1^2 D_2^2} \varepsilon^\lambda \varepsilon^\tau \text{tr} \left( \not{q}_2 \not{k} \gamma_\lambda (1 - \gamma_5) \not{l} \not{q}_1 (\not{l} - \not{q}_1) \not{q}_1 \not{l} \gamma_\tau (1 - \gamma_5) \not{k} \not{q}_2 (\not{k} + \not{q}_2) \right) \\
&= \frac{2f(M_W)}{D_1^2 D_2^2} z \alpha_1 \beta_2 s q_1^2 q_2^2 \varepsilon^\lambda \varepsilon^\tau \text{tr} \left( \not{k} \gamma_\lambda^\perp \not{l} \not{l} \gamma_\tau^\perp (1 - \gamma_5) \not{k} \right) \\
&= \frac{8f(M_W)}{D_1^2 D_2^2} \alpha_1 \beta_2 s q_1^2 q_2^2 k^2 l^2
\end{aligned} \tag{A.1.8}$$

$$\begin{aligned}
\text{and where } \sigma(M_W) &= 4(4\pi\alpha_S(M_W))^2 \sqrt{2} G_F M_W^2 \left( \frac{N_c^2 - 1}{2N_c} \right)^2 \frac{1}{4N_c} \\
D_1 &= k^2 - m_u^2 = \alpha_k \beta_k s - k_\perp^2 - m_u^2 \\
D_2 &= l^2 - m_d^2 = \alpha_l \beta_l s - l_\perp^2 - m_d^2
\end{aligned} \tag{A.1.9}$$

where in the last step,  $\gamma_5$  anticommutes past 4 gamma matrices in the trace, to give a  $(1 - \gamma_5)^2 = 2(1 - \gamma_5)$  term. We use the fact that the part of the trace on the RHS of Eq. (A.1.7), which contains a  $\gamma_5$  matrix can be removed, because evaluating the part of the trace containing the  $\gamma_5$  matrix gives a result which is antisymmetric in  $\mu$  and  $\rho$ , which contracted with the symmetric term  $p_1^\mu p_1^\rho$ , gives zero.  $\varepsilon^\lambda$  and  $\varepsilon^\lambda$  are the polarisation vectors of the final state W bosons in Fig. 5. In Eq. (A.1.7), we use the fact that

$$\varepsilon^\lambda \varepsilon^\tau = g^{\lambda\tau} \tag{A.1.10}$$

and using the integration measure

$$\int \frac{d^4 k}{(2\pi)^4} \int \frac{d^4 l}{(2\pi)^4} = \frac{s}{2} \int d\alpha_k d\beta_k \frac{d^2 k_\perp}{(2\pi)^4} \frac{s}{2} \int d\alpha_l d\beta_l \frac{d^2 l_\perp}{(2\pi)^4} \tag{A.1.11}$$

then Eq. (A.1.7) simplifies to

$$\begin{aligned}
A(\text{Fig. 5}) &= \frac{(4\pi\alpha_S(q^2))^2}{q_1^4 q_2^4 \alpha_1^2 \beta_2^2} \frac{s}{2} \int d\alpha_k d\beta_k \frac{d^2 k_\perp}{(2\pi)^3} \frac{s}{2} \int d\alpha_l d\beta_l \frac{d^2 l_\perp}{(2\pi)^3} H \\
&\times \delta\left(-\beta_k \alpha_1 s - \left(\vec{k} - \vec{q}_1\right)_\perp^2 - m_u^2\right) \delta\left(\alpha_l \beta_2 s - \left(\vec{l} + \vec{q}_2\right)_\perp^2 - m_d^2\right)
\end{aligned} \tag{A.1.12}$$

Using all the  $\delta$  functions to evaluate the relevant integrations, specifically taking the integral over  $\alpha_1 > \alpha_l$  and over  $\beta_2 > \beta_k$ , and using Eq. (A.1.1), we obtain

$$\begin{aligned} \frac{d\sigma^{BA}}{dY_W} &= \frac{\alpha_S^2(q^2)}{q_{1,\perp}^2 q_{2,\perp}^2} \sigma(M_W) \\ \text{where } \sigma(M_W) &= \left( \frac{N_c^2 - 1}{2 N_c} \right)^2 \frac{1}{4 N_c} \frac{\alpha_S^2}{4 \pi^3} \sqrt{2} G_F \ln \left( \frac{M_W^2}{4 m_u^2} \right) \ln \left( \frac{M_W^2}{4 m_d^2} \right) \end{aligned} \quad (\text{A.1.13})$$

It should be stressed, that the factor  $\alpha_S^2(q^2) / (q_{1,\perp}^2 q_{2,\perp}^2)$ , is included in the exchange of the BFKL Pomeron, or in more general words, it should be absorbed in the product of the two gluon functions  $x_1 G(q_1^2, x_1) x_2 G(q_2^2, x_2)$  that give the flux, (luminosity) of the gluons from both protons. The origin of the logs in Eq. (A.1.13), comes from the integrations over  $k_\perp$  and  $l_\perp$ . These integrations take the following form

$$\int d^2 k_\perp k_\perp^2 \left( \text{from the tr}(\dots) \right) \frac{1}{D_1^2} = \pi \ln(M_W^2/4m_u^2) \quad (\text{A.1.14})$$

## A.2 The amplitude for subprocess $GG \rightarrow b\bar{b}$

In this appendix, we calculate the amplitude for the subprocess  $GG \rightarrow b\bar{b}$ , in the region of large values of  $b\bar{b}$  mass, (denoted by  $M_{b\bar{b}} \approx M_H$ ). For such large values of the  $b\bar{b}$  mass, we can restrict ourselves by finding the contribution of the order of  $\ln(M_{b\bar{b}}^2/4m_b^2)$ , which stems from the simple diagram of Fig. 6. The cross section can be calculated using the following expression

$$\begin{aligned} M_{b\bar{b}}^2 \frac{d^2 \sigma^{BA}}{dM_{b\bar{b}}^2 dY_{b\bar{b}}} &= \frac{1}{4s} A \left( \text{Mueller amplitude (see Fig. 6) for the processes } p + p + [b\bar{b}] \rightarrow p + p + [b\bar{b}] \right) \\ &\times M_{b\bar{b}}^2 \delta(\alpha_1 \beta_2 s - M_{b\bar{b}}^2) \delta \left( \frac{1}{2} \ln(\alpha_1/\beta_2) - Y_{b\bar{b}} \right) \end{aligned} \quad (\text{A.2.1})$$

The amplitude for this diagram is given by the expression

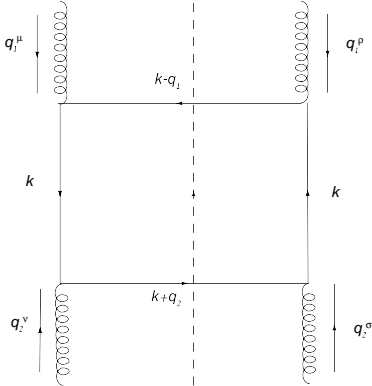
$$\begin{aligned} A(\text{Fig. 6}) &= \int \frac{d^4 k}{(2\pi)^4} \frac{(-ig_s)}{q_1^2} \bar{u}(p_1, s_1) \gamma^\mu u(p'_1, s'_1) \frac{(-ig_s)}{q_2^2} \bar{u}(p_2, s_2) \gamma^\nu u(p'_2, s'_2) \\ &\times \left( \frac{(-ig_s)}{q_1^2} \bar{u}(p_1, s_1) \gamma^\rho u(p'_1, s'_1) \frac{(-ig_s)}{q_2^2} \bar{u}(p_2, s_2) \gamma^\sigma u(p'_2, s'_2) \right)^\dagger S_{\mu\nu\rho\sigma} \end{aligned} \quad (\text{A.2.2})$$

Using Eq. (A.1.5) and Eq. (A.1.6), we find



$$\begin{aligned}
A(\text{Fig. 6}) &= \frac{4\pi\alpha_S}{\alpha_1^2 q_1^4} \frac{4\pi\alpha_S}{\beta_2^2 q_2^4} \int \frac{d^4 k}{(2\pi)^4} S \\
\text{where } S &= \frac{(4\pi\alpha_S (M_{b\bar{b}}))^2}{(k^2 - m_b^2)^2} q_{1,\perp}^\mu q_{1,\perp}^\rho q_{2,\perp}^\nu q_{2,\perp}^\sigma \text{tr} \left\{ (\not{k} - \not{q}_1 + m_b) \gamma_\rho (\not{k} + m_b) \gamma_\sigma (\not{k} + \not{q}_2 + m_b) \gamma_\nu (\not{k} + m_b) \gamma_\mu \right\} \\
&\times (2\pi)^2 \delta \left( (\vec{k} - \vec{q}_1)^2 - m_b^2 \right) \delta \left( (\vec{k} + \vec{q}_2)^2 - m_b^2 \right) \left( \frac{N_c^2 - 1}{N_c} \right)^2 \frac{1}{4N_c}
\end{aligned} \tag{A.2.3}$$

In Eq. (A.2.3), we have used the Sudakov expansion



$$\begin{aligned}
\vec{k} &= \alpha_k \vec{p}_1 + \beta_k \vec{p}_2 + \vec{k}_\perp \\
\vec{q}_1 &= \alpha_1 \vec{p}_1 + \beta_1 \vec{p}_2 + \vec{q}_{1\perp} \\
\vec{q}_2 &= \alpha_2 \vec{p}_1 + \beta_2 \vec{p}_2 + \vec{q}_{2\perp}
\end{aligned} \tag{A.2.4}$$

To calculate the trace in the expression for  $S$  given in Eq. (A.2.3), we recall that at high energy, the horizontal on mass shell  $b$  quarks in Fig. 9, have momentum which depend mostly on the longitudinal direction, and the vertical virtual  $b$  quark propagators, have momentum which depend mostly on the transverse direction. This observation reduces the RHS of Eq. (A.2.3) to the following expression

**Figure 9:** The process  $G + G \rightarrow b + \bar{b}$ .

$$\text{tr} \left\{ (\not{k} - \not{q}_1 + m_b) \not{q}_{1,\perp} (\not{k} + m_b) \not{q}_{2,\perp} (\not{k} + \not{q}_2 + m_b) \not{q}_{2,\perp} (\not{k} + m_b) \not{q}_{1,\perp} \right\} = 4\alpha_1 \beta_2 s q_1^2 q_2^2 (k^2 + m_b^2) \tag{A.2.5}$$

In terms of the Sudakov parametres introduced in Eq. (A.2.4), the integration measure of the  $k$  momentum space, becomes

$$\int \frac{d^4 k}{(2\pi)^4} = \frac{s}{2} \int \frac{d^2 k_\perp d\rho d\lambda}{(2\pi)^4} \tag{A.2.6}$$

Using Eq. (A.2.6), we integrate Eq. (A.2.2) over all the  $\alpha$ -s and  $\beta$ -s, taking into account the  $\delta$ -functions in Eq. (A.2.1). The result is given by the following expression

$$\begin{aligned}
M_{b\bar{b}}^2 \frac{d^2 \sigma^{BA}}{dM_{b\bar{b}}^2 dY_{b\bar{b}}} &= \frac{\alpha_S^2(q^2)}{q_{1,\perp}^2 q_{2,\perp}^2} \sigma(M_{b\bar{b}}) \\
\text{where } \sigma(M_{b\bar{b}}) &= \left( \frac{N_c^2 - 1}{2N_c} \right)^2 \frac{1}{16 N_c} \frac{\alpha_S^2}{8\pi} \frac{1}{M_{b\bar{b}}^2} \ln \left( \frac{M_W^2}{4m_b^2} \right)
\end{aligned} \tag{A.2.7}$$

where the log term has the same origin as in Eq. (A.1.14).

### A.3 The amplitude for the inclusive Higgs production via subprocess $GG \rightarrow H$

The expression for the cross section for the inclusive Higgs production process shown in Fig. 10, is very similar to the process of the  $W$  production due to gluon fusion, and it is equal to

$$\frac{d\sigma^{BA}}{dY_H} = \frac{1}{4s} A(\text{Mueller diagram of Fig. 10 for the process } p p H \rightarrow p p H) \delta\left(\frac{1}{2} \ln(\alpha_1/\beta_2) - y_H\right) \quad (\text{A.3.1})$$

The amplitude for this process shown in Fig. 10, is given by

$$A(\text{Fig. 10}) = A^2 \Pi_{\mu\nu} \Pi_{\rho\sigma} \frac{(4\pi\alpha_S(q^2))^2}{q_1^4 q_2^4} \times \sum_{\text{spins}} \{ \bar{u}(p'_1) \gamma^\mu u(p_1) \bar{u}(p'_2) \gamma^\nu u(p_2) \} \{ \bar{u}(p'_1) \gamma^\rho u(p_1) \bar{u}(p'_2) \gamma^\sigma u(p_2) \}^\dagger \quad (\text{A.3.2})$$

$$\text{where } A^2 = \frac{4\sqrt{2}G_F\alpha_S^2(M_H)}{9} (N_C^2 - 1) \quad \text{and} \quad \Pi^{\mu\nu} = q_1^\nu q_2^\mu - \frac{M_H^2}{2} g^{\mu\nu} \quad (\text{A.3.3})$$

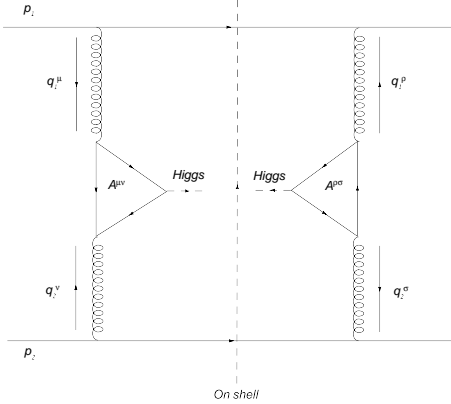


**Figure 10:** The process of inclusive Higgs production due to gluon fusion:  $G + G \rightarrow Higgs$ .

Using Eq. (A.1.5) and Eq. (A.1.6), as well as the form of the gauge invariant tensor  $\Pi^{\mu\nu}$ , we readily obtain the following expression after integration over the  $\alpha$ -s and  $\beta$ -s

$$\frac{d\sigma^{BA}}{dY_H} = \frac{\alpha_S^2(q^2)}{q_{1,\perp}^2 q_{2,\perp}^2} \sigma(M_H) \quad \text{where} \quad \sigma(M_H) = \left( \frac{N_c^2 - 1}{4N_c^2} \right) \frac{A^2}{256\pi} \quad (\text{A.3.4})$$

Since the Pomeron exchange, or more specifically the gluon structure functions enter in the same way for the case of the  $b\bar{b}$  pair production, as in the case for Higgs production due to gluon fusion, we can calculate the ratio

$$\frac{M_{bb}^2 \frac{d^2\sigma(p+p \rightarrow [b\bar{b}] + X)}{dM_{bb}^2 dY_{b\bar{b}}}}{\frac{\sigma(p+p \rightarrow H + X)}{dY_H}} = \frac{\sigma(M_{b\bar{b}})}{\sigma(M_H)} \quad (\text{A.3.5})$$

Using Eq. (A.2.7) and Eq. (A.1.13), we have

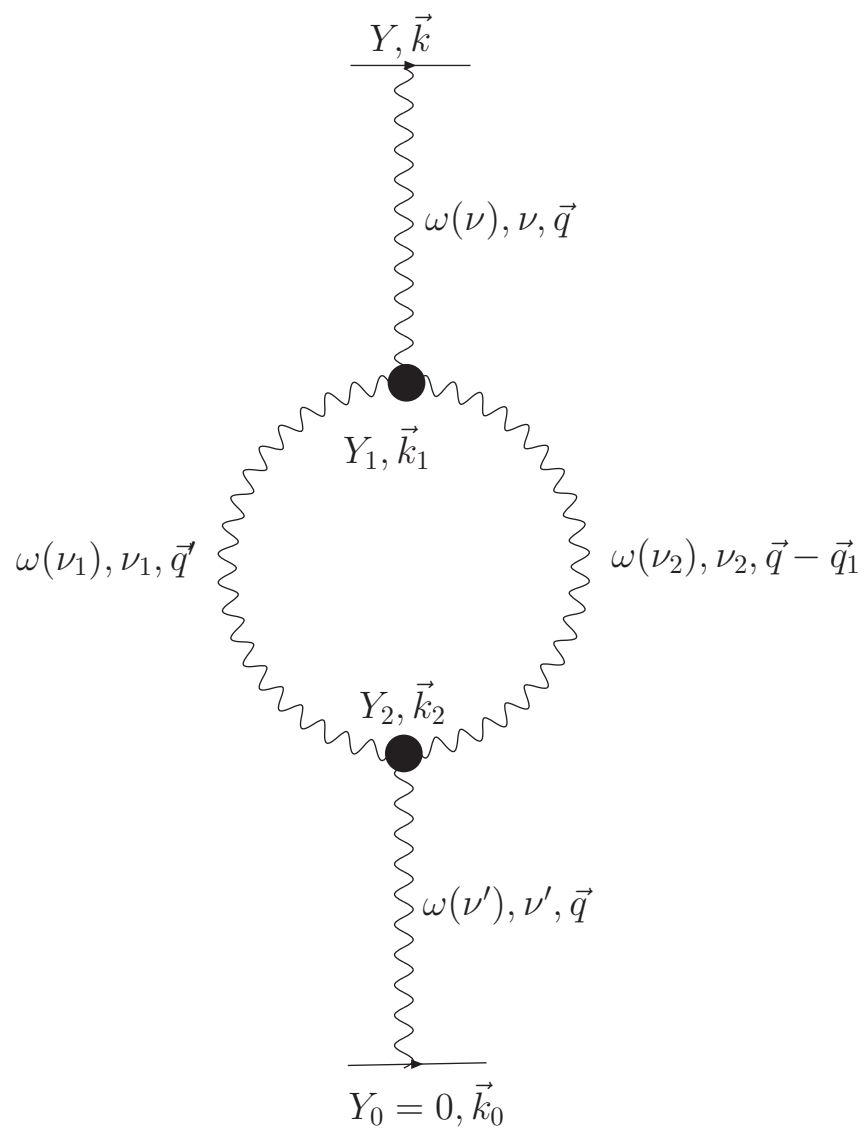
$$M_{bb}^2 \frac{d^2\sigma(p+p \rightarrow [b\bar{b}] + X)}{dM_{bb}^2 dY_{b\bar{b}}} = \frac{4}{3} \frac{32\alpha_S^2}{M_{bb}^2 A^2} \ln(M_{bb}^2/4m_b^2) \times \frac{d\sigma(p+p \rightarrow H+X)}{dY_H} \quad (\text{A.3.6})$$

where the factor of 4/3 is a colour factor.

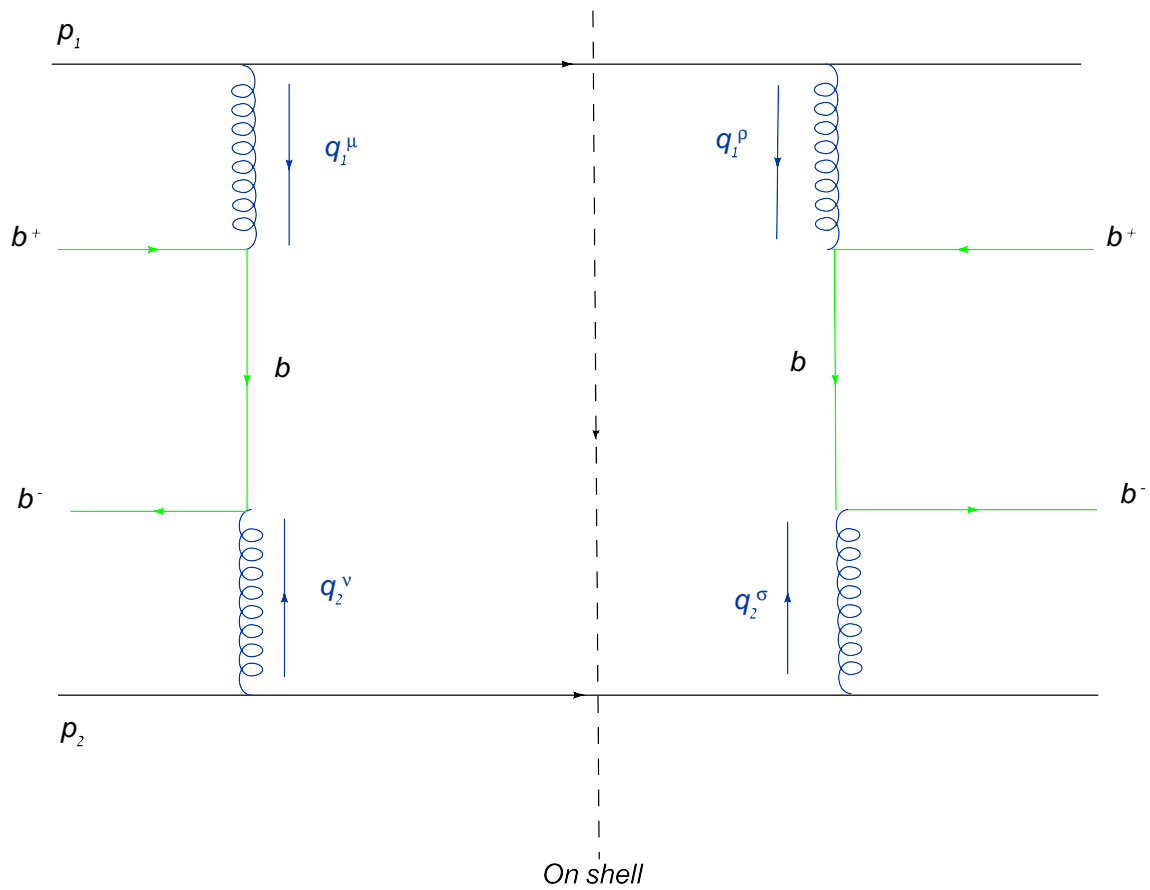
## References

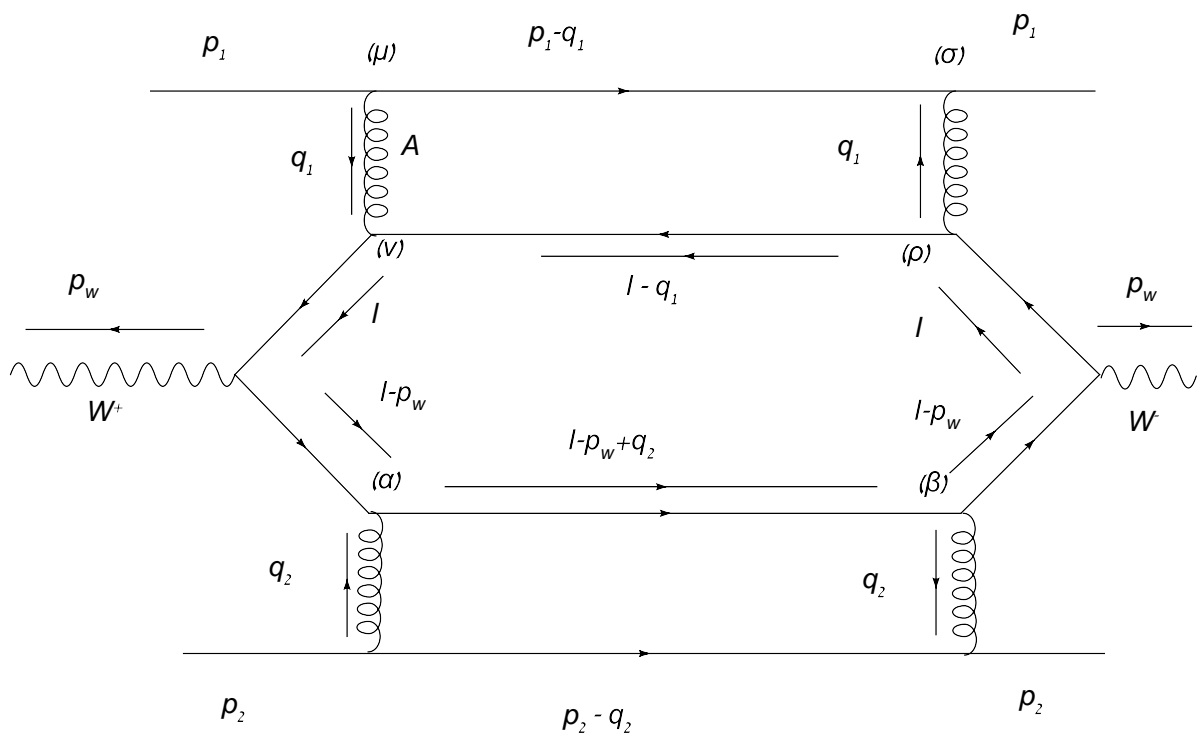
- [1] V. A. Khoze, A. D. Martin and M. G. Ryskin, arXiv:0705.2314 [hep-ph] and references therein.
- [2] P. V. Landshoff, “The total cross section at the LHC,” arXiv:0709.0395 [hep-ph], arXiv:hep-ph/0509240; A. Achilli, R. Hegde, R. M. Godbole, A. Grau, G. Panzeri and Y. Srivastava, “Total cross-section and rapidity gap survival probability at the LHC through an eikonal with soft gluon resummation,” arXiv:0708.3626 [hep-ph]; K. Igi and M. Ishida, “Predictions of p p, anti-p p total cross section and rho ratio at LHC and cosmic-ray energies based on duality,” arXiv:hep-ph/0510129, Phys. Lett. B **622** (2005) 286 [arXiv:hep-ph/0505058]; G. Matthiae, “Total cross-section and luminosity,” Eur. Phys. J. C **4S1** (2002) 13.
- [3] F. Abe *et al.* [CDF Collaboration], Phys. Rev. D **56**, 3811 (1997); Phys. Rev. Lett. **79**, 584 (1997).
- [4] J.C. Collins, D.E. Soper and G. Sterman: Nucl. Phys. **B308**, 833 (1988).
- [5] S. Catani, M. Ciafaloni and F. Hautmann, Nucl. Phys. **B366**, 135 (1991). E. M. Levin, M. G. Ryskin, Y. M. Shabelski and A. G. Shuvaev, Sov. J. Nucl. Phys. **53**, 657 (1991) [Yad. Fiz. **53**, 1059 (1991)]; J. C. Collins and R. K. Ellis, Nucl. Phys. **B360**, 3 (1991).
- [6] V. A. Abramovsky, V. N. Gribov and O. V. Kancheli, *Yad. Fiz.* **18**, 595 (1973) [*Sov. J. Nucl. Phys.* **18**, 308 (1974)].
- [7] E. A. Kuraev, L. N. Lipatov, and F. S. Fadin, *Sov. Phys. JETP* **45**, 199 (1977); Ya. Ya. Balitsky and L. N. Lipatov, *Sov. J. Nucl. Phys.* **28**, 22 (1978).
- [8] E. Levin, J. Miller and A. Prygarin, arXiv:0706.2944 [hep-ph].
- [9] A. H. Mueller, Phys. Rev. D **2**, 2963 (1970); Phys. Rev. D **4**, 150 (1971).
- [10] E. M. Levin and M. G. Ryskin, Phys. Rept. **189** (1990) 267; E. Laenen and E. Levin, *Nucl. Phys.* **B451** (1995) 207; *Ann. Rev. Nucl. Part. Sci.* **44** (1994) 199. [arXiv:hep-ph/9503381]; M. Gyulassy and L. McLerran, *Phys. Rev.* **C56** (1997) 2219; Y. V. Kovchegov and K. Tuchin, Phys. Rev. D **65** (2002) 074026 [arXiv:hep-ph/0111362];
- [11] V. N. Gribov and L. N. Lipatov, Sov. J. Nucl. Phys **15** (1972) 438; G. Altarelli and G. Parisi, Nucl. Phys. **B 126** (1977) 298; Yu. I. Dokshitzer, Sov. Phys. JETP **46** (1977) 641.
- [12] L. V. Gribov, E. M. Levin and M. G. Ryskin, *Phys. Rep.* **100**, 1 (1983); A. H. Mueller and J. Qiu, *Nucl. Phys.*, 427 **B 268** (1986) ; L. McLerran and R. Venugopalan, *Phys. Rev.* D **49**, 2233, 3352 (1994); D **50**, 2225 (1994); D **53**, 458 (1996); D **59**, 09400 (1999).

- [13] J. Bartels, M. Braun and G. P. Vacca, *Eur. Phys. J.* **C40**, 419 (2005) [arXiv:hep-ph/0412218]; J. Bartels and C. Ewerz, *JHEP* **9909**, 026 (1999) [arXiv:hep-ph/9908454]; J. Bartels and M. Wusthoff, *Z. Phys.* **C66**, 157 (1995); A. H. Mueller and B. Patel, *Nucl. Phys.* **B425**, 471 (1994) [arXiv:hep-ph/9403256]; J. Bartels, *Z. Phys.* **C60**, 471 (1993).
- [14] M. A. Braun, *Phys. Lett.* **B632** (2006) 297 [arXiv:hep-ph/0512057]; arXiv:hep-ph/0504002; *Eur. Phys. J.* **C16**, 337 (2000) [arXiv:hep-ph/0001268]; *Phys. Lett. B* **483** (2000) 115 [arXiv:hep-ph/0003004]; *Eur. Phys. J. C* **33** (2004) 113 [arXiv:hep-ph/0309293]; *Eur. Phys. J.* **C6**, 321 (1999) [arXiv:hep-ph/9706373]; M. A. Braun and G. P. Vacca, *Eur. Phys. J.* **C6**, 147 (1999) [arXiv:hep-ph/971114].
- [15] P. Nason *et al.*, “Bottom production,” arXiv:hep-ph/0003142; R. Bonciani, S. Catani, M. L. Mangano and P. Nason, *Nucl. Phys. B* **529** (1998) 424 [arXiv:hep-ph/9801375]; S. Frixione, M. L. Mangano, P. Nason and G. Ridolfi, *Adv. Ser. Direct. High Energy Phys.* **15** (1998) 609 [arXiv:hep-ph/9702287], *Nucl. Phys. B* **431** (1994) 453.
- [16] S. Marsini, R. D. Ball, V. Del Duca, S. Forte and A. Vicini, “*Higgs production via gluon-gluon fusion with finite top mass beyond next-to-leading order*”, arXiv: 0801.2544[hep-ph] and reference therein; “*Inclusive Higgs boson production at hadron colliders at next-to-leading order*”, arXiv: hep-ph/0205152; W.-M. Yao et al. (Particle Data Group), *J. Phys. G* **33**, 1 (2006) and 2007 partial update for the 2008 edition.
- [17] R. Hamberg and W. L. van Neerven, *Nucl. Phys. B* **379** (1992) 143; T. Matsuura, R. Hamberg and W. L. van Neerven, *Nucl. Phys. Proc. Suppl.* **23B** (1991) 3; *Nucl. Phys. B* **345** (1990) 331; C. Anastasiou, L. J. Dixon, K. Melnikov and F. Petriello, *Phys. Rev. D* **69** (2004) 094008 [arXiv:hep-ph/0312266]; K. Melnikov and F. Petriello, *Phys. Rev. Lett.* **96** (2006) 231803 [arXiv:hep-ph/0603182] and references therein.
- [18] P. Nason, S. Dawson and R. K. Ellis, *Nucl. Phys. B* **303**, 607 (1988), *Nucl. Phys. B* **327**, 49 (1989); M. L. Mangano, P. Nason, and G. Ridolfi, *Nucl. Phys. B* **373**, 295 (1992).
- [19] J. R. Ellis, M. K. Gaillard and D. V. Nanopoulos, *Nucl. Phys. B* **106**, 292 (1976); A. I. Vainshtein, M. B. Voloshin and V. I. Zakharov, *Sov. J. Nucl. Phys.* **30**, 431 (1979); The Review of Particle Physics W.-M. Yao et al., *Journal of Physics, G* **33**, 1 (2006) and 2007 partial update for 2008.











A Feynman diagram showing a vertical wavy line (photon) interacting with a horizontal fermion line. The fermion line consists of two parallel horizontal lines with arrows pointing to the right. The left end of the fermion line is labeled  $x_{12}$ . The right end is labeled  $E_q^{n,\nu}(x_{12})$ . The wavy line is attached to the top of the fermion line, and its upper end is labeled  $\vec{q}$ .

$$\begin{array}{c}
 \vec{q}, \vec{k}, \nu \\
 \text{wavy line} \\
 \nearrow \quad \searrow \\
 \vec{x}_1 \quad \vec{x}_2 \\
 \text{straight lines} \\
 \nwarrow \quad \swarrow \\
 \vec{q} - \vec{q}_1, \vec{k}, \nu_1 \quad \vec{q}_1, \vec{k}, \nu_2
 \end{array}
 =
 \begin{array}{c}
 \text{wavy line} \\
 \bullet \\
 \nwarrow \quad \swarrow \\
 \text{wavy lines}
 \end{array}
 \Gamma(\vec{q}, \vec{q} - \vec{q}_1, \vec{q}_1; \vec{k} | \nu, \nu_1, \nu_2)$$